Journal of Geophysical Research: Oceans

RESEARCH ARTICLE
10.1029/2018JC013866

Future Wave Conditions of Europe, in Response to High-End Climate Change Scenarios

Lucy M. Bricheno[1] **and Judith Wolf**[1]

[1]National Oceanography Centre, Liverpool, UK

Key Points:
- Dynamically downscaling wave model improves period and direction but not significant wave height
- Future mean significant wave height around Europe projected to decrease by 10%
- Extreme significant wave height can increase by up to 1 m, but projections have higher uncertainty

Correspondence to:
L. M. Bricheno,
luic@noc.ac.uk

Citation:
Bricheno, L. M., & Wolf, J. (2018). Future wave conditions of Europe, in response to high-end climate change scenarios. *Journal of Geophysical Research: Oceans*, *123*, 8762–8791. https://doi.org/10.1029/2018JC013866

Received 31 JAN 2018
Accepted 1 NOV 2018
Accepted article online 6 NOV 2018
Published online 5 DEC 2018

Abstract Changes in future North Atlantic storminess will impact upon wave conditions along the European coasts, with implications for coastal erosion, overtopping, and flood risk. In this study we make a detailed analysis of historic and future wave conditions around the European Atlantic coast, making projections out to the year 2100 under Representative Concentration Pathways 4.5 and 8.5 future emissions scenarios. A decrease in mean significant wave height of the order 0.2 m is projected across most of the European coast. Increases in the annual maximum and 99th percentile wave height as large as 0.5–1 m are observed in some areas but with a more complex spatial pattern. An increase in waves to the north of Scotland is also observed, mainly caused by a reduction in sea ice. We generate a set of coastal wave projections at around 10-km resolution around continental Europe, Ireland, and the British Isles. Widening of the probability density function (PDF) is observed, suggesting an increased intensity of rare high wave events in the future. The emergent signal of a reduced mean wave height is statistically robust, while the future changes in extreme waves have a wider confidence interval. An assessment of different extreme waves metrics reveals different climate change response at very high percentiles; thus, care should be taken when assessing future changes in rare wave events.

Plain Language Summary Waves are important to shipping, coastal flooding, and erosion. A numerical model of waves was built and tested for skill in representing historic waves, by comparing against observations at buoys. Climate model winds were then used to drive a model of sea surface waves. The future projections show a decrease in average wave height but increases in the maximum waves. The statistical method used to measure extreme waves seen during storms can affect the conclusion. We see evidence that the mean can go down, while the extremes increase in future.

1. Introduction

Coastal areas (less than 100 m above sea level) are the most densely populated on Earth — currently, with more than 35% of the world's Gross Domestic Product and 40% of the population is located there (Rosen, 2000). The Low Elevation Coastal Zone (less than 10 m above sea level) contains 10% of the world's population and 13% of the world's urban population (McGranahan et al., 2007). The relevant physical variables which can affect the coastline, potentially causing flooding and erosion in a warmer future climate, are global/regional sea level rise and changes in extreme sea levels, storminess, and waves. Interactions with stakeholders (such as fisheries and coastal planners) have highlighted the importance of understanding future changes in waves under high-end climate change. Castelle et al. (2018) show that winter wave height around Europe has increased significantly since 1984, as well as variability in wave conditions. Large/long-period waves are the most damaging for overtopping (Palmer et al., 2014). Large short steep waves are most damaging for navigation, offshore fishing, and marine transport. Therefore, we must examine changes in extreme waves as well as more typical conditions.

Projections of mean sea level rise have been well studied, and the contribution from different components (thermal expansion, glaciers, ice sheets, etc.) is relatively well understood (Jevrejeva et al., 2017). The contribution of waves to the sea-level jigsaw has often been neglected. Melet et al. (2018) found that water level changes due to wave setup largely exceed the contribution from thermal expansion and large-scale ocean dynamics. However, changes in storminess, and thus surge and wave conditions, are harder to predict with confidence, due to the large interannual and decadal variability in synoptic weather conditions (Palmer & Hagedorn, 2006). Storm surges, driven by low atmospheric pressures and high winds, are largely localized and controlled by local weather and coastal geometry (Wolf, 2009). Waves, on the other hand, are generated by a

combination of local and nonlocal forcing. Locally, high winds will drive short, steep waves (wind sea), while large nonlocal swells can travel long distances across ocean basins. Waves integrate the effect of winds over the fetch across which they blow, and thus, there may still be changes in waves where no significant change in wind speed occurs (Wolf & Woolf, 2006), due to changes in duration or direction of the wind. In this work we use a dynamical downscaling approach to investigate changes in wave climate around Northwest (NW) Europe in response to future winds and ice cover.

Wave climate may be defined as the statistics and probability of occurrence of wave parameters, such as wave height, period, and direction, usually over some period for which they may be regarded as representative for a particular location (Wolf et al., 2011). The natural variability in wave climate is large (IPCC et al., 2013). In order to identify any robust change, we choose to examine coastal impacts of climate change for high-end emission scenarios, that is, where global average warming is projected to exceed 2 °C with respect to preindustrial temperatures. Errors in wave models can largely be attributed to errors in the forcing wind fields. Therefore, we need to use the most reliable atmospheric models to provide winds fields for this study. Our best source of knowledge for future atmospheric forcing is global climate models (GCMs), which may then be downscaled to more appropriate resolution for coastal applications, using regional climate models (RCMs). Downscaling uses global-scale projections, using accepted greenhouse gas (GHG) emissions scenarios to generate regional forecasts, with increased spatial and temporal resolution. This downscaling from global to regional projections is vital for the study of meaningful local impacts (Wolf et al., 2015), until higher-resolution global models are computationally possible.

One of the outstanding issues is to demonstrate how added value is provided by dynamical downscaling, and many studies over the last 10 years have addressed this question. The climate models have been run for the historical period as well as future projections, and the former allows an assessment of the accuracy of the models, by comparison with observations and reanalyses, such as ERA-Interim (Dee et al., 2011). Giorgi and Gutowski (2015) review the issue of added value from RCMs with reference to the CORDEX (Coordinated Regional Climate Downscaling Experiment) initiative, a World Climate Research Programme Project which has carried out systematic dynamical downscaling for 13 regions and suggests ways forward. Kotlarski et al. (2014) assess the performance of the EURO-CORDEX model ensemble for temperature and precipitation and could not clearly demonstrate added value from the regional downscaling; however, Donat et al. (2010) explore the benefits and limitations of dynamical downscaling for windstorm loss calculations and, in general, found a distinct advantage from dynamical downscaling. Kunz et al. (2010) found that all RCMs tend to underestimate the magnitude of the gusts in a range between 10% and 30% for a 10-year return period. They find spatial resolution to be less important over areas of homogeneous terrain (including over water), stating that over regional seas, including the North and Baltic Seas, the driving global model is controlling the wind fields. Bricheno et al. (2013), however, demonstrated the benefits of high-resolution winds for coastal modeling. Menendez et al. (2014) show that while no benefit in model accuracy is shown for regional downscaling in the open Atlantic, improved accuracy is obtained in coastal waters and in the Mediterranean.

Vousdoukas et al. (2017) highlight waves as a very important component of extreme sea level and present projections of regional climate change out to 2100. The variability is large, with no clear direction of change. They also note that there is still no consensus within the literature regarding projections of future wave conditions around the European coast. Similarly, Mentaschi et al. (2017) found that the coast of the British Isles contained areas where the trends in projected wave energy were opposing, suggesting that the regional seas were highly spatially varying, and not well connected with climate patterns. Hemer et al. (2013) describe analysis of an ensemble of global wave projections, which has been made publicly available by the Coordinated Ocean Wave Climate Project community (www.jcomm.info/cowclip), which aims to generate and share wave climate projections. They find an agreed projected decrease in annual mean significant wave height (SWH) over 25.8% of the global ocean area (including the North Atlantic) which is greater during Boreal winter (January–March) than austral winter. Hemer and Trenham (2016) show that high performance of GCMs for *standard* climate variables does not imply high performance for GCM-forced wave simulations. Camus et al. (2017), using weather typing and statistical downscaling, informed by a historical data set of wave data, showed how this method could be used to provide high-resolution coastal impact assessment, including additional variables such as wave period and direction as well as SWH. Their results show that the global multimodel projections of the SWH and peak period are consistent with changes obtained in previous studies, that is, a decrease in mean wave height and peak period for the North Atlantic. The main disadvantage of the

methodology is that it is not able to estimate hourly future wave conditions to force process-based impact models.

Previous wave projection with the wave model WAM, forced by the HadCM3 ocean-atmosphere GCM downscaled with the atmosphere-only HadRM3 RCM using SRES scenarios, is described by Wolf et al. (2015). The model forcing included the Met Office/Hadley Centre perturbed parameter ensemble, in which different parameter settings in the climate model, and their effect on climate sensitivity, were explored. The future climate storm track was seen to be displaced to the south over the United Kingdom/NW Europe, leading to an increase in wave heights to SW of the United Kingdom and a decrease to the north of Scotland. The wave model was run for 140 years from 1960 to 2100 for the unperturbed ensemble member and for 20-year time slices (1960–1990 and 2070–2100) for the perturbed members. Brown et al. (2012) used these wave model projections (as well as the surge projections) at a single location to examine the likely changes in extreme waves in Liverpool Bay, in the eastern Irish Sea. They found that future trends in the wave projections closely follow those of the winds, since waves in Liverpool Bay are locally generated. In general, they found a reduction in mean monthly winds and waves. Trends in large (>3 m) and extreme (>5 m) wave events, defined as the peak height of an isolated wave event (with successive events separated by at least 12 hr), were investigated, and in both cases a positive trend is found. Extreme wind and wave conditions were projected to become less frequent but with the most severe becoming more intense, with a projected increase of 9.5% from the present-day value of 5.34 m $\pm$ 0.98 m. Most large wave events are close to the 3-m level, with an extreme 7.09-m level being achieved once during the study period (in 2084). However, the magnitude of the projected change is small compared with the annual variability in the wave heights. Some work has recently been done in preparing wave climate projections for Ireland (Gallagher et al., 2016), which is exposed on its west coast to large waves from the North Atlantic. They use a three-member ensemble of EC-Earth to force the WaveWatch III^{TM} model, using a set of three nested grids for the North Atlantic, with an unstructured grid for the nearshore waters around Ireland, including the Irish Sea. For this area the model predicts an overall decrease in annual and seasonal mean SWH around Ireland, corresponding to an average decrease in mean surface wind speeds, with the largest decreases in summer (up to 15%) off the south coast and winter (up to 10%) off the west coast for Representative Concentration Pathway (RCP)8.5, with smaller changes for RCP4.5. Zacharioudaki et al. (2011) investigate changing waves in North East Atlantic, using two future climate models. They find a reduction in mean and 99th percentile SWH at the end of the century compared to present-day conditions. The mean is seen to decrease more strongly, with the largest reductions seen to the west of the Iberian Peninsular. There is more uncertainty in the changes to the 99th percentile, but the spatial patterns are similar. Lionello and Sanna (2005) found that wave heights have been decreasing in various parts of the Mediterranean Sea during the second half of the twentieth century. Lionello and Giorgi (2007) used wind fields computed by regional climate simulations for the period 2071–2100 to find a reduction of wave height in November, December, and May under increased GHG forcing. Aarnes et al. (2017) evaluate an ensemble of wave models around NW Europe, projecting a decrease in mean wave height in most areas (though potentially an increase in areas of melting sea ice). They also predict that there will be increased uncertainty in extreme wave climate in the future.

Aarnes et al. (2017) evaluate changing wave conditions in the Northeast Atlantic, forced by six different climate models (including EC-Earth, used here). Our work has elements in common with this approach, and we would like to acknowledge their contribution as informative to this study. The wave model of Aarnes et al. (2017) had a focus on the Northeast Atlantic (encompassing part of the Arctic and Norwegian Seas) and was run at 50-km resolution. In our work, we have focused on downscaling a single model to provide information at the coast, at a high resolution (below 10-km resolution). This work adds to the current knowledge with a focus on NW Europe, considering the mean and extreme wave conditions. Our exploration of future wave conditions examines the full PDF and makes projections for the whole NW European coast, extending to 35°N in the south. In the present study we aim to answer three questions:

- Does dynamical downscaling add value to wave projections?
- Are there significant changes in projected future wave climate (mean and extreme)?
- How does changing wave climate manifest itself at the coast?

The remainder of the paper first discusses the state of the art in climate and wave modeling in section 2, in order to select a well-performing climate model for forcing the wave model. In section 3 we describe a new model configuration and the experiments run with it. In section 4, validation results from this model are pre-

sented and we compare the performance of the global and regional model, by validation against observations over the historical period, before examining future changes in wave climate in section 5. We focus on changes at the coast in section 6 and extreme wave climate in section 7 which are useful outputs for coastal planners. All results are discussed in section 8, and conclusions drawn in section 9.

2. Selection of a Climate Model for Wave Model Forcing

In this study we used dynamical models to study the behavior of waves around NW European coasts, which requires a large amount of computational effort, compared to studies done by statistical downscaling methods (e.g.,Camus et al., 2017). Therefore, we decided to choose one well-tested GCM with good performance over NW Europe rather than using several models in an ensemble. While a limited ensemble may give a wider spread of results, it still may not capture all of the uncertainty in wave model projections, some of which is due to limitations common to all GCMs in terms of the model physics and coarse resolution.

As surface waves are driven by sea surface winds, the performance of the climate models in simulating winds requires assessment before the most suitable is used to force the wave model. The state of the art in climate modeling is assessed by the World Climate Research Programme Coupled Model Intercomparison Project (CMIP), CMIP5 (Taylor et al., 2012), which builds upon the previous phase, CMIP3. There are biases in the performance of CMIP5 models over the North Atlantic (Dee et al., 2011), and even the models with good present-day validation can diverge in their projections of future storm tracks. Perez et al. (2014) examine the skill of CMIP3 and CMIP5 models, specifically over the NE Atlantic region and conclude that the most skilled GCMs in the study region are UKMO-HadGEM2, ECHAM5/MPI-OM, and MIROC3.2 (hires) for CMIP3 scenarios and ACCESS1.0, EC-Earth, HadGEM2-CC, HadGEM2-ES, and CMCC-CM for CMIP5 scenarios. In parallel, Zappa, Shaffrey, and Hodges (2013) subdivided the CMIP5 models into three groups by means of their performance in reproducing North Atlantic extratropical cyclones. The best performing group, with only small biases in winter time position and median latitude (consistent with reanalysis data), includes EC-Earth, GFDL-CM3, HadGEM2-ES, and MRI-CGCM3. EC-Earth and HadGEM2-ES thus appear to perform best in both studies, which is also confirmed in Masato et al. (2013).

The models available in CMIP5 have a coarse resolution (typically 1° latitude by 1° longitude) and so do not resolve tropical cyclones and poorly resolve midlatitude storms (de Winter et al., 2013). The CMIP5 future projections of North Atlantic cyclones for the end of the 21st century have been assessed by numerous authors (Harvey et al., 2012; Mizuta, 2012; Chang et al., 2013, Zappa, Shaffrey, Hodges, et al.2013). Assessment of the CMIP5 model performance suggests that EC-Earth, MIROC, and MOHC (HadGEM2) perform best over Europe for winter and the National Center for Atmospheric Research model performs best in the summer. (Masato et al., 2013). To supplement the coarse-resolution models, EC-Earth has been used at high resolution (≈25 km, 91 vertical levels) to investigate changes in midlatitude storms in response to greenhouse warming (Haarsma et al., 2013). The occurrence of hurricane force winds (>32.6 m/s) has been found to increase over Western Europe and occurs earlier in the season, from August to October, due to a rise in Atlantic tropical sea surface temperatures which is extending the breeding ground of tropical cyclones eastward. In addition to more frequent and intense hurricanes reaching Europe, the shorter travel distance will increase the likelihood of these storms maintaining their tropical storm intensity (Haarsma et al., 2013). From the 19 CMIP5 GCMs with 44 different configurations, we selected the EC-Earth model (Hazeleger et al., 2012) for the wave model forcing. This model has been found to be one of the top-performing models for Europe, with low biases and good skill over the NE Atlantic, as well as performing well during the winter months when extreme waves will be generated. As the model has performed well historically, it is reasonable to use this model as a source of driving data for wave modeling in this work.

What changes do these state-of-the-art climate models predict for future winds and storminess over the North Atlantic? The two most important factors to consider are the strength of wind and the position of the storm track, and how they will change in future. The Adaptation Sub-Committee of the Committee on Climate Change (ASC) (2015) report develops a high-impact, low-probability scenario (termed H++) for wind storms over the United Kingdom based on an analysis of the CMIP5 model projections. It finds that the CMIP5 climate model projections suggest a plausible H++ scenario for a 50–80% increase in the days of strong winds over the United Kingdom by 2070–2100 compared to the period 1975–2005. In general, the ensemble of models projects a southerly shift in the storm track over NW Europe. In 2012, the previous Climate Change Risk Assessment Evidence Report (Wade et al., 2013) described the potential impacts of climate change based largely on the UKCP09 projections.

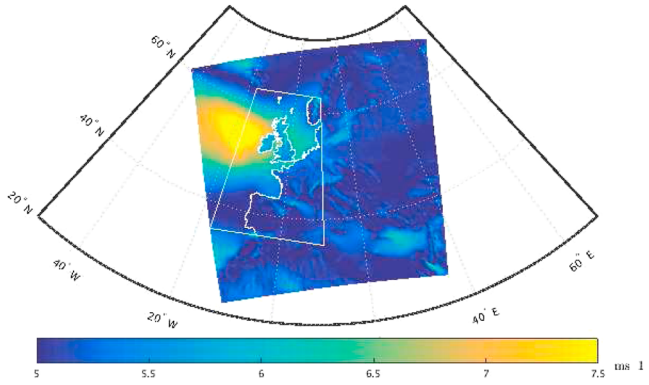

Figure 1. Monthly mean wind speed (m/s) for January 1970 from Euro-Coordinated Regional Climate Downscaling Experiment atmospheric model domain (colored) and regional model grid extent (white box, with coastline highlighted).

Most climate models are still deficient in their representation of blocking over Europe, and this may be significant in not allowing storms to propagate correctly. Some studies have noted a tendency for reduced occurrence of blocking under future scenario conditions (e.g., Barnes et al., 2012). This response is closely related to the mean state changes (de Vries et al., 2013; Woollings, 2010), which, in general, comprise strengthened westerly winds although this result has considerable uncertainty; (e.g.,Woollings & Blackburn, 2012). In Masato et al. (2013) a winter poleward shift in high-latitude blocking and an eastward summer shift are identified. In summer, the decrease in blocking is accompanied by a poleward storm track shift into the high-latitude blocking region. This may mean that the incidence of blocked storms will increase. By the end of the 21st century, model analysis over Europe indicates a 30% decrease in blocked days during winter (although not over Eastern Europe) and a 35% increase in blocked days during summer for Europe to western Russia. Zappa et al. (2014) show that biases in winter European blocking frequency are related to the North Atlantic storm track tilt and Mediterranean cyclone density. Zappa et al. (2015) show that a climate-related signal emerges sooner (10–20 years) from the natural variability if seasonal averages rather than an annual mean are used to examine the climate response. This suggests that by considering extreme, winter waves, we may be able to see emergent signals more easily than by looking at the annual means. As a result of this assessment and its availability as a GCM and an RCM in Euro-CORDEX, the EC-Earth model was selected as being a well-performing model, although still subject to limitations experienced by all models for North Atlantic storms (Flato et al., 2013).

3. Wave Model Setup and Methods for Global and European Projections

For the present work, the WaveWatch III^{TM} spectral wave model version 3.14 (Tolman, 2009), hereafter WW3, has been used to investigate changing wave conditions globally and in the North Eastern Atlantic. Two model implementations were set up using WW3: a global wave model domain and a nested domain covering the North East Atlantic. The global configuration consists of a Spherical Multiple Cell grid with a resolution of 0.703° (longitude) × 0.469° (latitude), extending from ≈ 80°N to 80°S. Rather than focusing solely on NW Europe, the regional model was extended to the south in order to cover the full Atlantic-facing coast of the Iberian Peninsula. The extent of the regional model is highlighted in white in Figure 1. The wave model is configured to use 36 directional bins (giving a directional resolution of 10°) and 30 frequency bins, using a logarithmic distribution, with a minimum frequency of 0.04118 Hz. Source terms described in Tolman and Chalikov (1996), representing energy input and dissipation by bottom friction, depth-limited wave breaking and whitecapping, were chosen following on from a comparison made by Cannaby et al. (2015). JONSWAP was used for dissipation by bottom friction and Battjes and Janssen for depth-limited breaking, with the dissipation constant set to the default value of 1. The breaking parameter, gamma $(\gamma) = -0.038$. Unresolved islands are represented by a partial obstruction to the propagating wave energy as detailed by Tolman (2003). Ice in the global model was represented as a fractional cover between 0 and 1.

The regional North East Atlantic model was run on a regular latitude-longitude grid at 0.083° × 0.083° (less than 9 km) resolution. The wave physics configuration and direction and frequency resolution are configured as for the global model. The reason for the selection of the regional resolution is that it has been used in several previous studies (e.g., Brown et al., 2010) and found to be satisfactory, without the need for an intermediate step. The 1/12th° regional resolution is used frequently for U.K. surge model and wave studies. It also follows the downscaling of GCM to RCM, and there is no available forcing at an intermediate scale. Full wave spectra produced by the global mode are provided to the regional domain at the open boundaries at an hourly frequency. There is no ice cover in the regional model.

3.1. Atmospheric Model Forcing

To investigate future climates, the wave model forced RCP scenarios as defined by the International Panel for Climate Change assessment (IPCC et al., 2013). The RCP scenarios each represent a different level of GHG emissions, leading to a certain amount of surface heating in 2100. RCP4.5 is a stabilization scenario, where the radiative forcing is stabilized before 2100. RCP8.5 is characterized by radiative forcing that increases more

Table 1
Locations of Buoy Data Used for Wave Model Validation and the Start Date of Observations, Together With the Number of Records Used at Each Site

Buoy	Latitude	Longitude	Start date	End date	N Recs
Poole	50°38′.02N	1°43′.13W	17 December 2003	Present	106,730
Liverpool	53°32′.01N	3°21′.30W	13 November 2002	Present	101,910
Moray	57°57′.98N	3°19′.99E	29 August 2008	Present	61,350
Hebrides	57°17′.53N	7°54.85W	23 February 2009	Present	35,060
Scilly	49°49′.00N	6°32.78W	11 October 2014	25 March 2016	10,720
S. Knock	51°34′.23N	1°34.76E	15 January 2010	5 February 2016	50,403
Belmullet A	54°17.08′N	10°16.21′W	15 January 2010	Present	92,696
Belmullet B	54°14.03′N	10°8.57′W	15 December 2009	17 April 2015	771,720
Belmullet C	54°13.50′N	10°5.52′W	10 September 2014	17 April 2015	7,980
K1	48°42.00′N	12°24.00′W	5 January 2006	Present	159,956
K2	51°00.00′N	13°30.00′W	5 January 2006	Present	164,799
K4	54°31.80′N	12°21.00′W	5 January 2006	Present	120,791
K5	59°06.00′N	11°24.00′W	5 January 2006	Present	120,791
K7	60°42.00′N	4°30.00′W	5 January 2006	Present	72,181
7341	36°29.38′N	6°57.77′W	1 November 2006	Present	106,443
17330	39°30.60′N	9°38.40′W	1 June 2011	Present	21,585
7302	43°53.35′N	3°48.95′W	1 August 2007	Present	52,640
7334	47°48.95′N	2°47.22′W	1 January 2010	Present	65,812
7336	45°54.98′N	1°50.02′W	1 March 2014	Present	18,377
8916	54°55.13′N	8°00.53′E	1 December 2011	Present	12,039
602	58°29.00′N	10°56.00′E	1 January 2010	Present	30,391
8705	53°36.83′N	4°57.64′E	1 November 2011	Present	196,374
8993	60°38.61′N	3°43.16′E	1 July 2014	Present	7,004

rapidly, it assumes business as usual with no GHG reduction up to 2100. Changes in near-surface wind speed are associated with a large spread among individual ensemble members at both warming levels. Kjellström et al. (2018) examined European climate change for global mean temperature increases of 1.5 and 2 °C above preindustrial conditions. They found that relatively large areas over the North Atlantic and some parts of the continent show decreasing wind speed, while some ocean areas in the far north show increasing wind speed.

The global model was forced by 3-hourly 10-m winds and daily sea ice cover from the EC-Earth model (run at the Swedish Meteorological and Hydrological Institute). EC-EARTH (Hazeleger et al., 2012) uses coupled ocean and atmosphere models, which are, respectively, the NEMO Version 2 (Madec, 2008) and the Integrated Forecasting System cycle 31r1 atmospheric model from ECMWF (http://www.ecmwf.int/research/ifsdocs/CY31r1/index.html). The atmosphere model is at 1.125° resolution. The ocean model is at ≈1° resolution, though this falls to 1/3° in equatorial regions. The ocean model also has three poles (South Pole, Canada, and Siberia) to improve resolution in the high-northern polar region. The preindustrial control run is 730 years long, though the other tests are initialized to begin at the end of this run. This could therefore be considered the spin-up period. There are 14 ensemble members for ocean, atmosphere, sea ice, and land-based parameters (historical and projections). Hazeleger et al. (2012) comment that the model performs well in simulating tropospheric fields and dynamic variables and performs less well in simulating surface temperature and fluxes. In common with all climate models, there is an issue with drift in some variables, in particular SST. Sen Gupta et al. (2013) show that, for EC-EARTH, globally averaged SST trends vary across the ensembles from 0.3 to 0.45 °C/50 years. The local SST drift ranges −0.04 to 0.02 °C/50 years.

Dynamical downscaling, using a combination for global and RCMs is recommended as the best approach for studying wave climate by, for example, Zacharioudaki et al. (2011). For the regional wave model forcing, we have chosen to use regional downscaled model winds from the CORDEX framework (Giorgi et al., 2009). Euro-CORDEX has produced an ensemble of high-resolution (0.11° and 0.44°) downscaled European RCMs, forced by GCMs from the CMIP5 project. The Euro-CORDEX simulations consider the global climate simula-

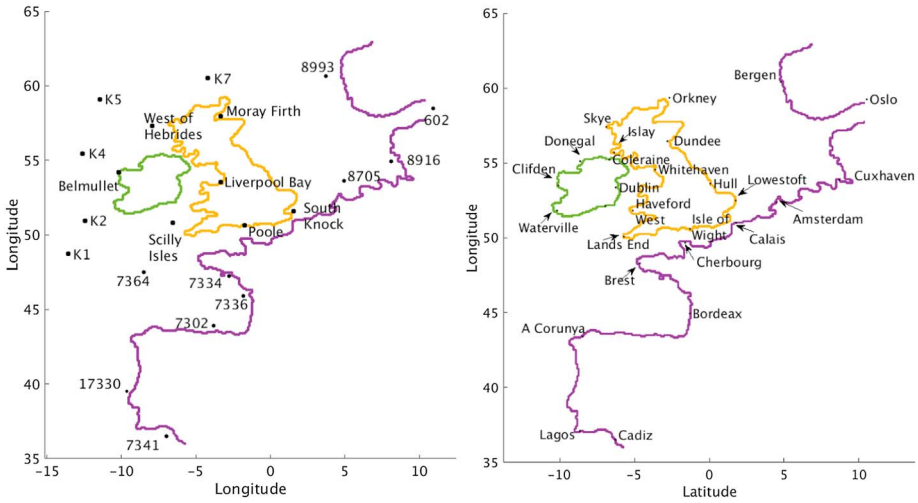

Figure 2. Locations of buoys used for validation (left) and coastal *strips* (right) where wave conditions are extracted, together with cities and coastal locations for orientation on Figures 10–12.

tions from the CMIP5 long-term experiments up to the year 2100. They are based on RCP4.5, RCP8.5, and RCP2.6 emissions scenarios Moss et al. (2010). These were provided by the SHMI's Rossby Centre regional atmospheric model (RCA4) and are described in Strandberg et al. (2015). For the baseline conditions, the RCA4 was run forced by global ERA-Interim model winds. While the global ERA-Interim product included data assimilation, the regional RCA4 runs do not. Historical and future scenarios run through RCA4 are also performed using the same regional model to downscale the EC-Earth GCM winds. Data may be accessed through the Earth System Grid Federation (https://esgf-index1.ceda.ac.uk/projects/esgf-ceda/). Our regional wave model domain was forced at the surface by a 6-hourly 10-m wind product of EUR-11 ICHEC-EC-EARTH Strandberg et al. (2015).

4. Wave Model Validation

4.1. ERA-Interim Versus Observations

As a baseline condition a recent past-/present-day climatology period was first simulated for the period 1970–2005. After 2005 the *future* scenarios diverge and we have investigated two possible scenarios: RCP4.5 and RCP8.5, in order to cover one extreme scenario and a more moderate future. The future wave projections have been run continuously from 2006 to 2100. However, as the present day refers to a model climatology (and not historical weather conditions), a hindcast has also been run forced by ERA-Interim winds (Dee et al., 2011) for the period 1979–2015. This hindcast period is first used to validate the model performance before any conclusions can be drawn about future wave conditions.

In order to provide confidence in the wave model results, the SWH, mean wave direction, and peak period were validated against observations for the hindcast period (1979–2015, with buoy data available from 2002). SWH was extracted at 23 sites (detailed in Table 1 and shown in Figure 2) representing a range of exposures and water depths. The hindcast historic run was compared with Met Office, Irish Marine Institute (http://data.marine.ie/), CEFAS WaveNet buoys (https://www.cefas.co.uk/cefas-data-hub/wavenet/), together with data made available from EMODnet (http://www.emodnet-physics.eu). The analysis was performed on the ERA-Interim forced models, both global (low resolution) and regional (high resolution) runs. The wave buoys are located in a range of water depths and exposures, with most recording up to the end of our validation period (a total of 2,402,994 records). The water depth and position in the model may not correspond exactly to the observation station in some places, but the closest model point to the buoy was chosen. The modeled and true water depths, as well as distance from buoy to modeled value, are shown in Table 2. To assess the model's representation of SWH, at each site we calculated a correlation coefficient (R^2), root-mean-square error (*r.m.s.e*) and a percentage model bias (*PBias*). This is defined by Marechal (2004) and Brown et al. (2010) as

Table 2
Modeled and True Water Depth and the Distance Between the Wave and Modeled Values

Buoy	Buoy depth	Global depth	Regional depth	Global distance	Regional distance
Poole	18 m	45 m	14 m	25.3 km	4.4 km
Liverpool	13 m	12 m	13 m	20.0 km	4.0 km
Moray	49 m	48 m	49 m	14.1 km	3.9 km
Hebrides	100 m	111 m	83 m	17.8 km	4.6 km
Scilly	90 m	100 m	92 m	10.5 km	3.2 km
Knock	26 m	27 m	19 m	28 km	1.4 km
Belmullet A	100 m	59 m	60 m	10.4 km	4.1 km
Belmullet B	50 m	59 m	27 m	4.9 km	2.4 km
Belmullet C	50 m	206 m	260 m	7.3 km	2.8 km
K1	1,070 m	999 m	1,902 m	27 km	4.5 km
K2	2,000 m	999 m	2,074 m	26 km	2.3 km
K4	2,800 m	999 m	1,583 m	32 km	4.0 km
K5	2,000 m	999 m	1,834 m	28 km	3.9 km
K7	650 m	917 m	1,079 m	8 km	3.7 km
7341	463 m	319 m	380 m	36.19 km	4.3 km
17330	2,085 m	656 m	1,248 m	19.77 km	3.17 km
7302	2,522 m	999 m	2,376 m	8.85 km	3.61 km
7334	35 m	15 m	34 m	38.95 km	4.28 km
7336	52 m	48 m	51 m	25.09 km	0.06 km
8916	14 m	10 m	16 m	17.68 km	0.72 km
602	500 m	125 m	271 m	14.29 km	48.14 km
8705	24 m	25 m	26 m	35.31 km	5.52 km
8993	304	273 m	299 m	17.70 km	4.25 km

Note. In the global wave model *deep* waters are set to 999 m.

$$\mathrm{PBias} = 100\frac{\sum_{n=1}^{N} M_n - D_n}{\sum_{n=1}^{N} D_n} \tag{1}$$

where M_n is the model prediction and D_n represents the data for a number of observations N. As well as assessing the modeled SWH, the mean wave direction and peak period (Tp) are also considered. The absolute error in modeled mean wave direction (degrees) is calculated with respect to observations; however, wave direction is not recorded at all buoy sites (e.g., Met Office *K* buoys). The complex error (*CErr*; e.g., Noye et al., 1999) can be used to find the magnitude of deviation from observed wave direction.

$$\mathrm{CErr} = \frac{2\pi}{360}\sqrt{(\cos\theta_M - \cos\theta_O)^2 + (\sin\theta_M - \sin\theta_O)^2} \tag{2}$$

where θ_M is the modeled wave direction and θ_O is the observed wave direction. Additionally, the circular standard deviation (v) is calculated as defined by Mardia and Jupp (2009) as

$$v = \sqrt{-2\ln(\bar{R}_1)} \tag{3}$$

where $\bar{R}_1$ is the resultant length of a series of unit vectors, each representing the difference between modeled and observed direction. If all samples share the same direction, the resultant vector (R) will have length close to 1 and the circular variance be small. This is calculated using the MATLAB toolbox described in Berens (2009). As shown in Table 2, for most sites the water depth is well represented; however, the water depth at Belmullet C, for example, is significantly deeper in the model than reality. This may go some way to explaining why the SWH at Belmullet C (in 56 m of water) is significantly overpredicted with a PBias of 22.80% in the global model (water depth 206 m).

The model performs best in deep water and swell dominant sites (K buoys and western approaches such as Scilly, 7032, 7336). The poorest performance is seen at wind sea-dominated sites in the North Sea, such

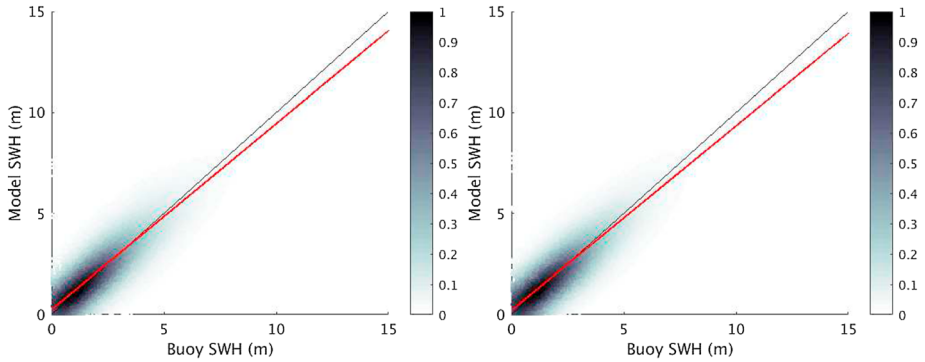

Figure 3. Density scatter plots of *SWH* (m) from the global model (left) and regional model (right), comparison of modeled (*y* axis) and observed data (*x* axis). The 1:1 line is plotted in black and a linear fit to data in red. SWH = significant wave height.

as South Knock, 8705, 8916, and 602. An overview comparison of the observed buoy and modeled SWH is presented as a binned scatter plot following the methodology of Carr et al. (1987), shown in Figure 3. A linear regression (plotted in red) $D_m = \alpha D_b + \beta$ is fitted to the modeled SWH. Where D_m is the model data and D_b the buoy data, and the 1:1 line is also shown in black. The global wave model returns $\alpha = 0.92$ and $\beta = 0.24$; in the regional model, $\alpha = 0.91$ and $\beta = 0.20$; that is, a slightly better correlation in the global model but smaller bias in the regional model. This fit demonstrates an underprediction in the most extreme wave heights in both model configurations. This is not unexpected as the simulated winds tend to underestimate extreme events, due to the coarse atmospheric model grid missing small-scale (in space and time) features.

The average r.m.s.e for the coarse model is 0.72 m, reducing to 0.70 m in the regional model. There is also a modest improvement in the R^2 correlation, from 0.906 to 0.911, as the model resolution increases. The values of PBias are also similar: ±19.67% in the global model and ±19.61% in the regional model. To examine the model performance at contrasting sites, the individual buoy sites are considered separately. A detailed statistical validation of the SWH and mean direction is presented in Tables 3 and 4 for the global and regional models, respectively. Comparing the validation statistics in Tables 3 and 4, there is little to choose between the performance at low and high resolution. In fact, there is more variability and a slightly higher r.m.s.e at many sites in the high-resolution model. The largest model biases are seen at the sheltered sites of Liverpool Bay, Moray Firth, and Poole Harbour. The regional model has a large underprediction at these sites; however, as this is a relative error, this may also be a function of the smaller wave height observed at these sites. It is important to note that the global winds from EC-Earth contain data assimilation, while the regional Euro-Cordex model is free running with no assimilation. This may explain some deterioration in the quality of the results where the waves are fetch limited and therefore more dependent on the quality of modeled winds.

In order to assess the model's skill in representing the mean and extreme wave conditions, the 50th and 99th percentiles are compared in Table 5. To summarize this, we consider some bulk statistics at the 23 buoy sites. For the 50th percentiles in the global model $R^2 = 0.97$; $R^2 = 0.99$ in the regional model. In the global model r.m.s.e = 0.11 m, and r.m.s.e = 0.04 in the regional model. PBias = +5.0% in the global and +1.5% in the regional model. Turning to extreme waves, for the 99th percentile, the global model has r.m.s.e = 0.09 m, and the regional model 0.04 m. The PBias in the global model is +3.3% and -0.34% in the regional model. The R^2 correlation is 0.98 in the global and 0.99 in the regional model. This shows that both models are capable of representing both mean and extreme wave conditions reasonably well, with an improvement in all metrics when model resolution is increased.

Model resolution has a more significant impact on wave direction than on SWH. In seven out of nine sites analyzed the wave direction is better modeled with high resolution (though the modeled standard deviation is still large, due to the inherent variability). This improvement is particularly strong at shallow, sheltered sites including Liverpool Bay and the Moray Firth. Figure 4 shows directional wave roses for two sites where model resolution leads to improved representation of wave direction. In the Moray Firth (top row Figure 4), the regional model is better able to capture the multidirectional wave spectra. Similarly, in the bottom row (Belmullet), the high resolution model better represents the narrow range of wave directions seen at this buoy.

Table 3
Validation Statistics for Coarse-Resolution Global Model SWH and Wave Direction Against Available Wave Buoy Data

Buoy	SWH R^2	SWH r.m.s.e (m)	SWH PBias (%)	*CErr* (°)	*v* (°)
Poole	0.85	0.42	+8.44	41.74	33.11
Liverpool	0.80	0.41	−13.24	46.71	51.77
Moray	0.81	0.41	−7.31	41.88	76.45
Hebrides	0.76	1.17	+7.18	17.94	34.49
Scilly	0.94	0.50	+5.00	12.57	31.07
Knock	0.78	0.28	+4.54	34.35	66.64
Belmullet A	0.79	0.84	−5.45	22.98	39.00
Belmullet B	0.91	0.83	3.47	17.59	32.55
Belmullet C	0.92	0.77	22.80	18.17	9.27
K1	0.80	1.04	+1.28	—	—
K2	0.87	0.87	+2.61	—	—
K4	0.88	0.86	+2.10	—	—
K5	0.87	0.86	−0.46	—	—
K7	0.88	0.79	+2.46	—	—
7341	0.77	0.51	−18.54	—	—
17330	0.81	0.71	−1.41	—	—
7302	0.89	0.62	−4.76	—	—
7334	0.89	0.52	+24.55	—	—
7336	0.89	0.46	+0.73	—	—
8916	0.77	0.55	+26.34	—	—
602	0.80	0.57	−19.34	—	—
8705	0.86	0.50	+8.76	—	—
8993	0.76	1.14	+17.35	—	—
All sites	0.91	0.72	± 19.67%	28.21	41.59

Note. For SWH R^2 correlation, r.m.s.e, and PBias are shown. The mean complex error and standard deviation of wave direction are also shown. SWH = significant wave height; r.m.s.e = root-mean-square error; Pbias = percentage model bias; CErr = complex error.

The wave model must also be capable of representing the wave period, particularly the peak period (*Tp*) which is the more commonly observed parameter. *Tp* and SWH can be examined together as a bivariate scatter plot (e.g., Wolf et al., 2011; Tucker & Pitt, 2001). Figure 5 shows the *Tp* − *SWH* distributions for eight of the buoy sites, with observed conditions in black, and modeled (from the regional configuration) adjacent in red. The covariance of wave height and period can help classify the different sites, for example, the Scillies and Hebrides are dominated by swell waves, with large SWH and *Tp*, while the distribution of *Tp* and SWH at South Knock show that this site is fetch-limited, with small short-period wind-driven waves. By classifying the different buoy sites in this way, we see that the model is adequately representing the observed wave conditions at a range of different sites, exposures, and water depths. These scatter plots are from the regional model output, and should be considered in conjunction with statistics listed in table 4 to understand the associated R^2 correlation, PBias and r.m.s.e.

4.2. Present-Day Climatology

In order to be confident in the projections, we must also make a comparison between the historical modeled wave conditions (driven by ERA Interim reanalysis) and the recent past climate runs. Though historical climate model forcing is statistically similar, it does not represent actual events as seen in the ERA-Interim forced simulation. In this section, the average wave conditions have been compared at the buoys used for validation in section 4. The 30-year means from the historic run 1970–1999 are used from both the global and regional wave model integrations then compared with the full data set available at each buoy site. At some buoys, only

Table 4
Validation Statistics for Fine Resolution Regional Model SWH and Wave Direction Against Available Wave Buoy Data

Buoy	SWH R^2	SWH r.m.s.e (m)	SWH PBias (%)	*CErr* (°)	*v* (°)
Poole	0.84	0.51	−30.60	29.83	33.31
Liverpool	0.79	0.44	−13.64	30.55	49.67
Moray	0.70	0.56	−21.54	37.09	75.25
Hebrides	0.75	1.18	−2.34	17.69	37.16
Scilly	0.92	0.58	4.65	15.40	33.55
Knock	0.68	0.34	−0.36	37.59	70.59
Belmullet A	0.83	0.75	−5.56	18.67	38.73
Belmullet B	0.92	0.79	−0.17	11.66	33.10
Belmullet C	0.89	0.91	−8.50	3.52	9.37
K1	0.84	0.91	+1.02	—	—
K2	0.87	0.85	+2.60	—	—
K4	0.88	0.86	+2.06	—	—
K5	0.88	0.85	−1.81	—	—
K7	0.88	0.79	+2.43	—	—
7341	0.79	0.44	+2.29	—	—
17330	0.76	0.78	+2.22	—	—
7302	0.89	0.61	−1.70	—	—
7334	0.88	0.55	+22.85	—	—
7336	0.89	0.45	+4.91	—	—
8916	0.75	0.57	+25.77	—	—
602	0.76	0.58	−2.31	—	—
8705	0.77	0.60	+8.44	—	—
8993	0.69	1.02	+1.92	—	—
All sites	0.91	0.70	± 19.61%	22.24	42.30

Note. For SWH R^2 correlation, r.m.s.e, and PBias are shown. The mean complex error and standard deviation of wave direction are also shown. SWH = significant wave height; r.m.s.e = root-mean-square error; Pbias = percentage model bias; CErr = complex error.

truncated data sets are available, varying from 4 years in the west of Hebrides, to over 12 years at the Liverpool Bay site. The periods when observed SWH data are available are shown previously in Table 1.

By taking monthly averages of the maximum and mean SWH, we can build up a picture of the seasonal cycle at each buoy site. These monthly means are calculated at all 16 buoys for all four configurations: regional/global models forced by ERA/historic winds. Summary statistics describing the performance of these four configurations are presented in Table 6. The top panels of Figure 6 show a summary of the monthly mean for the global model forced by ERA interim winds (left) and the maximum waves in the regional configuration forced by historic climatology winds (right). All model configurations do a reasonable job of representing the monthly averaged wave climate, with R^2 correlations above 92% and biases below 15%. The r.m.s.e are of the order 0.35 m in the mean SWH and 1.1 m in the maximum SWH. The seasonality is better captured in the ERA model than the historic model (smaller r.m.s.e). We are confident that the seasonal cycle in both mean and maximum SWH is well represented, with small inherent bias observed in the climate-forced simulations.

To understand the (small) spatial biases present in the climate model EC-Earth, we can take 30-year averages of the wave conditions (mean and extreme) and compare the historic climate with the ERA-Interim reanalyis run. Comparable 30-year blocks are used to calculate model biases: 1975–2004 (ERA-Interim) and 1980–2009 (EC-Earth historic). The bottom panels of Figure 6 show maps of the percentage bias for the regional and global models. The global and regional models show similar spatial patterns of bias in the Atlantic, and both configurations have a positive bias. However, the mean is biased low in the global model in the Irish Sea and

Table 5
The 50th and 99th Percentile Validation Statistics at Observed Buoy Sites, Comparing Observations With Global and Regional Model Configurations

	50th percentile (m)			99th percentile (m)		
	Buoy	Global	Regional	Buoy	Global	Regional
Poole	0.8	0.91	0.57	1.03	1.12	0.71
Liverpool	0.71	0.63	0.59	0.89	0.77	0.73
Moray	0.94	0.93	0.73	1.11	1.03	0.86
Hebrides	2.56	2.81	2.52	2.99	3.20	2.92
Scilly	2.49	2.58	2.62	2.80	2.94	2.93
Knock	0.72	0.77	0.73	0.82	0.86	0.82
Belmullet A	2.60	2.51	2.42	2.85	2.69	2.29
Belmullet B	2.45	2.56	2.41	2.79	2.89	2.78
Belmullet C	2.72	3.58	2.71	3.10	3.81	2.84
K1	2.80	2.74	2.81	3.14	3.15	3.15
K2	2.80	2.88	2.90	3.20	3.28	3.28
K4	3.00	3.06	3.09	3.34	3.41	3.41
K5	3.10	3.11	3.06	3.46	3.46	3.40
K7	2.70	2.74	2.78	3.07	3.15	3.15
7341	1.05	0.82	1.08	1.20	0.98	1.22
17330	2.08	2.07	2.17	2.31	2.28	2.36
7302	1.76	1.72	1.76	2.12	2.02	2.09
7334	1.00	1.24	1.21	1.22	1.52	1.50
7336	1.50	1.55	1.64	1.77	1.78	1.86
8916	0.90	1.16	1.16	1.02	1.29	1.28
602	0.90	0.76	0.94	1.14	0.92	1.12
8705	1.19	1.31	1.33	1.38	1.50	1.50
8993	3.00	3.60	3.09	3.18	3.73	3.24

North Sea. The absolute mean percentage bias in the regional model is 5% for the mean and 10% for the maximum and 99th percentile. In the global model the absolute mean percentage bias is 7% for the mean, 10% for the maximum, and 8% for the 99th percentile. There does not appear to be any relationship between the distribution of high waves and larger biases. From this assessment we are confident that the EC-Earth *historic climate* runs are doing as good a job as the hindcast (ERA-Interim forced) simulations.

5. Results: Future Versus Recent Past

As explained in section 3, transient runs were performed, with the wave model running continuously from 2006 to 2100. There is a large degree of variability in the wave data, both observed and modeled. In order to make some comparisons between the present day and future waves, we now analyze the future wave climate by examining 30-year time slices. This approach was used to assess future wave climate by, for example, Hemer et al. (2013), under the Coordinated Ocean Wave Climate Project. Correspondingly, we have selected time slices to cover the recent past (1970–1999), midcentury (2030–2059), and end century (2070–2099).

A dynamical downscaling approach has been used in this work, which combines an improved representation of the local coastline and bathymetry with higher-resolution wind forcing. One added value of dynamical downscaling is the increased spatial resolution of the model output. This adds value in itself by giving a more fine-grained result which can be used for site-specific applications. Another benefit of the higher-resolution nested model is improved coastal resolution and fetch. It may be seen, for example, that higher waves penetrate into the Irish Sea and closer to the western coast of Ireland in the higher-resolution model. WW3 also has the capability to partially resolve missing land, that is, when small islands are underresolved, they are still parametrized, as a percentage blockage to passing wave energy (Tolman, 2003). Figure 7 compares seasonal

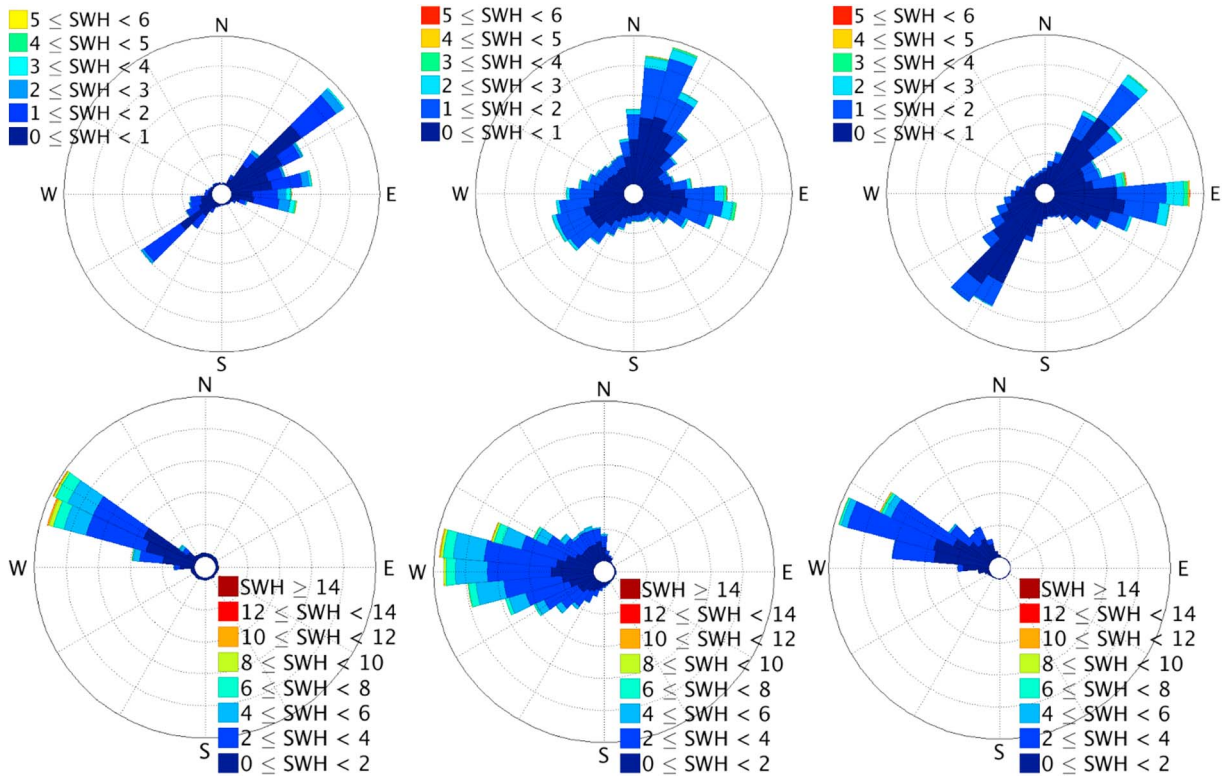

Figure 4. Wave roses representing historic wave climate from the buoy (left), global model (centre) and regional model (right). Two sites where the modeled wave direction was improved significantly by increased resolution: Moray Firth (top) and Belmullet (below).

future projections from the global and regional models. The results are broadly similar (as should be expected from a downscaled model: the patterns ought not be radically different).

Figure 7 shows differences in seasonal mean SWH between the recent past and end century from the RCP8.5 scenario. The maps focus on NW Europe, and compare seasonal mean SWH for 3-month averages over summer (June, July, August) and winter (December, January, February). Dynamical downscaling gives increased spatial resolution, especially close to the coast, and in semi-enclosed seas. Although dynamical downscaling leads to increased resolution of spatial features in the wind fields, we do not see an increase in peak wind speeds associated with these sharper features (not shown). The summer mean SWH shows changes of the order 0.10 m, with a reduction observed around 45–60°N. The SWH reduces more in the downscaled modeled future, by as much as 0.2 m in places. There is a slight increase in the summer mean South of 45°N, again of the order 0.1 m. A reduction in winter mean SWH is seen across most of the domain, and is particularly strong to the north west of the British Isles, by over 0.3 m. There are however some projected increases in SWH notably, with the semi-enclosed seas such as the Irish Sea and English Channel. These increases are seen more strongly in the regional model.

Wave height has a very large range, dependent on whether conditions are calm, or a storm is passing. This leads to a large variability in SWH, making any signal of change in wave conditions hard to identify from the noise. In order to separate out physical changes from a noisy background, statistical methods such as a Kruskal-Wallis (KW) test (Kruskal & Wallis, 1952) can be used. This is a non-parametric test to determine whether one sample is significantly different from another. Applying a KW test to compare a distribution of future wave height with the recent past, we can assess whether the modeled wave conditions have changed. In the results shown in Figures 8 and 9, a KW test is applied to two populations in order to mask out changes which are not statistically significant. Black shading is used where the KW test falls below 50%, gray shading indicates a KW test score of between 50% and 75%. Where the KW test score exceeds 75% the absolute differences between the historical and future wave conditions are shown. In these cases, we are confident that future wave conditions are statistically significantly different to past wave climate.

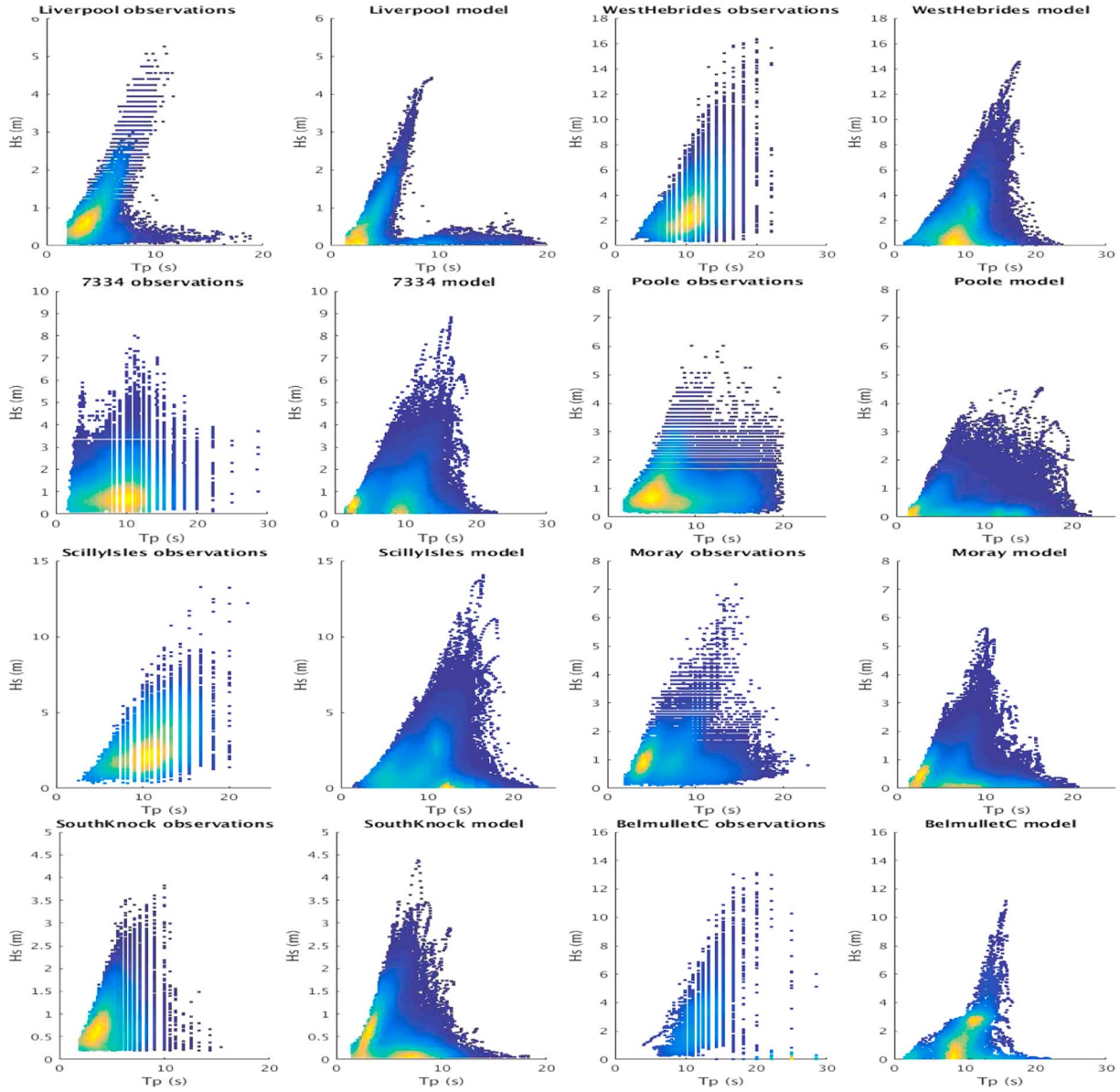

Figure 5. Bivariate histograms comparing observed peak period and SWH distribution at eight sites around the UK. Observations left and regional modeled in red right. The distributions are colored by occurrence, so that hot yellow colors imply a high density of wave spectra with these characteristics. The roses represent a the direction from which the waves approach.

Figure 6 shows the projected change in 30-year mean SWH. A reduction is shown across all futures in most of the domain, of the order 0.1 m. The largest reduction is seen in RCP8.5 by end century, with mean SWH lowered by 0.3 m off the west coast of Ireland. The exception is in the north of the domain, and can be seen most clearly in the mid-century RCP8.5 scenario; here, an increase in SWH is observed, which may be related to Arctic sea-ice retreat. We can confirm this by returning to the GCM and calculating the northern hemisphere winter sea-ice cover. In the historical model (1970–1999), during a three month period over December-February, 12.0% of our wave model domain is covered with sea-ice. This coverage is seen to decrease in the future RCP4.5 projection to 10.4% (2030–2059) and 9.3% (2070–2099). The decrease is more marked in the RCP8.5 projection to 9.8% (2030–2059) and 5.5% (2070–2099). It is interesting to note how large the masked areas are in each of these future maps, as in these areas any future trend signal is disguised by natural variability. In the unmasked areas, the change signal is robust, and we can identify more areas of statistically significant change moving from middle to end century. There is still a large degree of uncertainty in future changes in

Table 6
Summary of Seasonal Climatologies: Monthly Mean and Maximum for 16 Sites

	Monthly mean			Monthly maximum		
Configuration	R^2	r.m.s.e	% Bias	R^2	r.m.s.e	% Bias
Global ERA	0.96	0.35	11.21	0.95	1.14	12.82
Global historic	0.97	0.32	10.98	0.93	1.15	13.42
Regional ERA	0.96	0.39	13.81	0.95	1.08	14.98
Regional historic	0.97	0.35	11.98	0.92	1.02	12.75

Note. r.m.s.e = root-mean-square error.

North Sea waves in the middle of the 21st century, while a significant decrease is not observed until the final 30 years.

The mean annual maximum (AnnMax) aims to capture intense meteorological events that occur regularly every year (and not the most extreme values which would be characterized with longer return periods). Figure 6 shows the difference in 30-year AnnMax between end-century RCP8.5 and the historic period. In contrast with the relatively modest changes in seasonal mean SWH, the changes in extreme SWH can be larger than 0.5 m in places. However, the spatial patterns are also a lot more complex, as the extreme wave events are more closely related to individual storm events than the mean or prevailing winds. This larger degree of uncertainty is also picked out by the statistical KW test. In all four futures there are large areas of the domain where we are unable to distinguish (statistically) between the historic and future period. There is also more heterogeneity in the maps, with areas of both increased and decreased AnnMax SWH. These

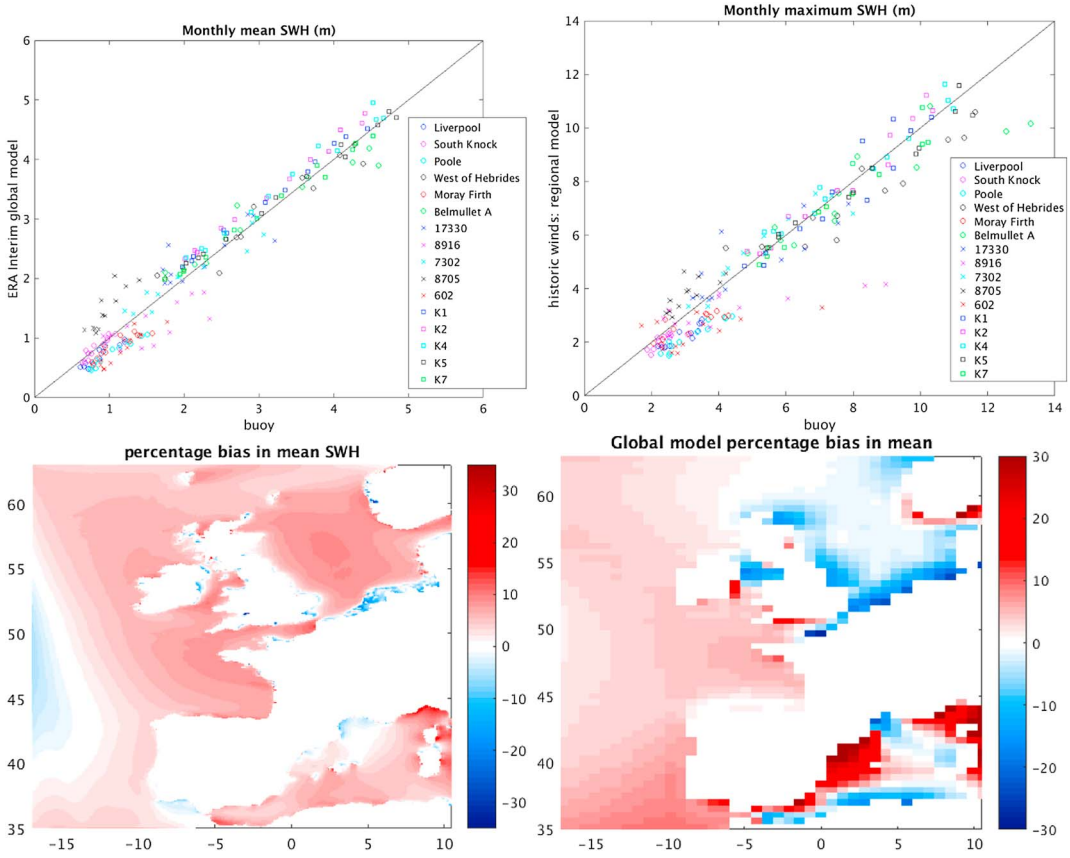

Figure 6. Scatter plots of average monthly mean (top left) and monthly maximum (top right) comparing buoy and modeled *SWH* at 16 sites. The global model forced by ERA interim winds is shown on the left and the regional configuration forced by historic climatology winds on the right. Maps of percentage bias in the regional model (lower left) and global model (lower right). SWH = significant wave height.

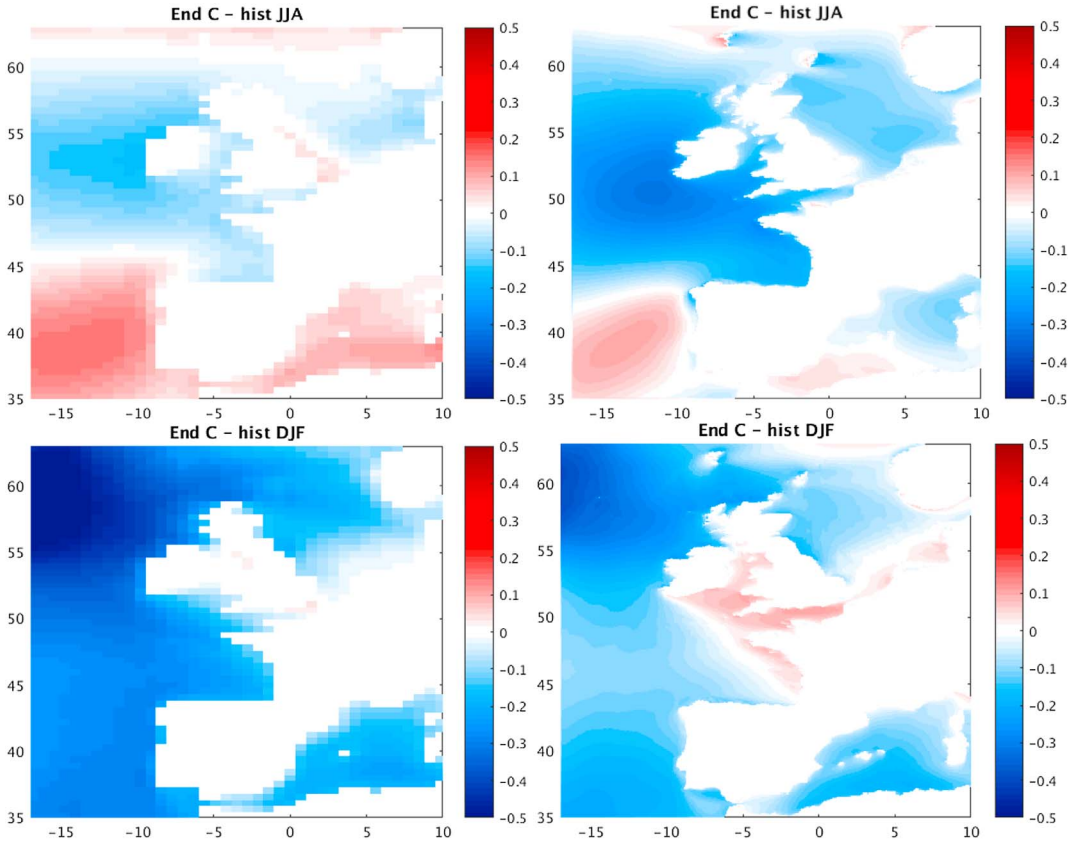

Figure 7. Projected change in seasonal mean SWH between present-day (1970–1999) and RCP8.5 future projections by end century (2070–2099). (top row) Summer (mean June, July, and August [JJA]). (bottom row) Winter (December, January, and February [DJF]). Results from global model integration (left) and regional model (right).

changes can be as large as 0.5 m, with larger areas experiencing an increase in extreme SWH (the opposite signal to the behavior of mean waves). On the east coast of the UK, extreme waves are project to decrease in the RCP8.5 scenarios, which is also seen in the lee of small island groups such as the Faroes, Shetland, and Orkney Islands. A robust increase in AnnMax SWH is observed in the SW of the domain next to the Iberian Peninsula. In all futures an increase in AnnMax is also seen in the north of the domain toward the Greenland / Iceland / Norwegian (GIN) Seas, related to sea ice (as explained earlier).

To conclude, projected changes (largely a reduction) in mean SWH are much more robust than changes in the extremes. The historic and future AnnMax SWHs are highly variable. However, future change signals are statistically significant in some areas. While largely positive, the direction of change is not spatially homogeneous (as it is for the mean), with AnnMax waves increasing in some areas and decreasing elsewhere. This illustrates the large variability in AnnMax SWH, and demonstrates a need to consider extreme events and internal natural variability when making predictions of future wave conditions. In the next section, a regional focus will be taken, in order to extract tangible outputs for planners, and those working at the coast.

6. Coastal Impacts

In order to focus on changing wave conditions close to the coast, the approach of Conte and Lionello (2013) and Lionello et al. (2017) has been adapted to provide similar outputs for the Atlantic coast of Europe and the NW European shelf, including the North Sea. The 30-year mean and AnnMax at each coastal point in the regional model have been extracted (providing ≈ 10-km separation along the coast). Figures (10–12) present the AnnMax wave height around the coast for three different coastlines (refer to Figure 2 for geographical context). In Figure 10, the Western European continental coast is shown from Norway to the Straits of Gibraltar along the horizontal axis. This format is repeated for the U.K. Mainland in Figure 11 and Ireland and Northern Ireland in Figure 12. Coastal waves will be influenced by local water depth, and the outputs shown here are

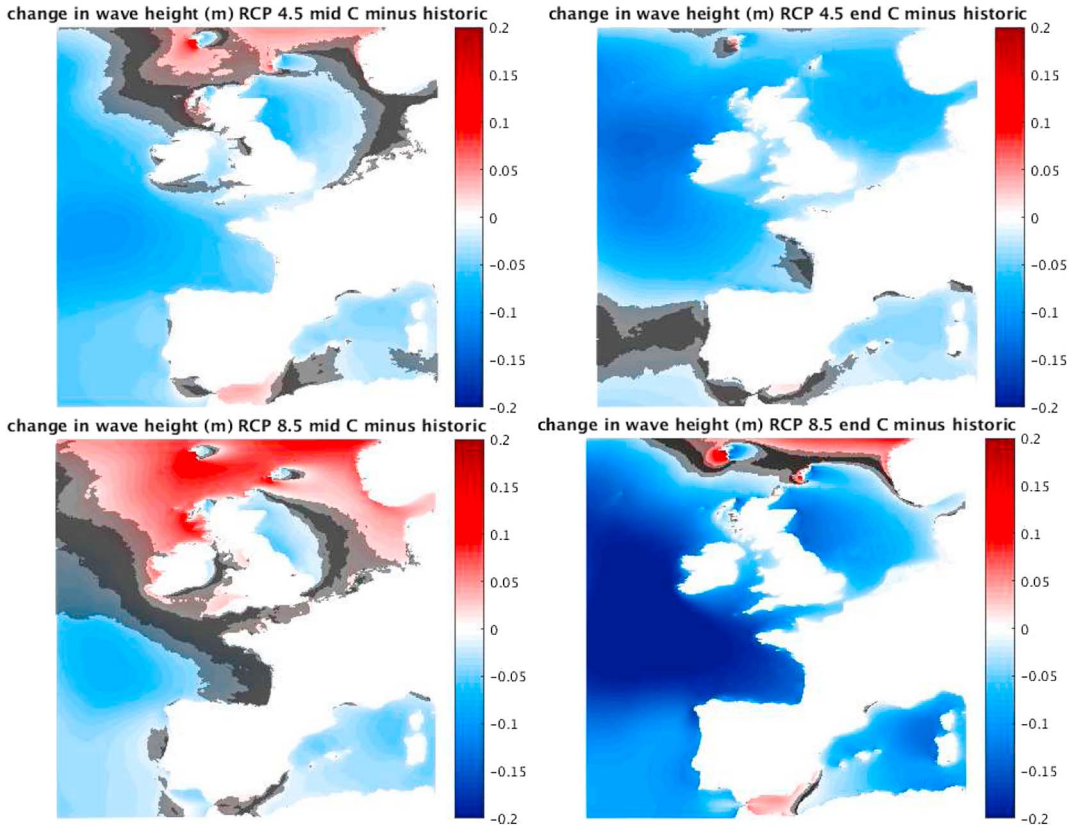

Figure 8. Projected changes in future mean SWH (m). Areas masked in black have a confidence below 50% and those masked in gray a confidence below 75%. (top row) RCP4.5. (bottom row) RCP8.5. (left) Middle century. (Right) End century. RCP = Representative Concentration Pathway.

extracted at locations with depths ranging from less than 10 m to more than 400 m. The water depths at coastal points are extracted and plotted along side the wave conditions in the first panel of Figures 10–12. In shallow water, wave heights may be depth limited (Battjes & Janssen, 1978); therefore, the wave conditions must be considered in combination with the local water depth. We can use a rule of thumb to calculate where in our model domain waves will be limited as $SWH > 0.4 * H$ where H is the water depth (plotted in the top panel of Figures 10–12). For the mean climate, this happens at 0.15% of the coastal locations, 4.7% (9.2%) of the locations when considering the 99th percentile (annual maximum). The second panels of Figures 10–12 show the mean and AnnMax coastal SWH for the present day. The lower two panels show relative changes in the future projections of mean and AnnMax SWH, respectively.

In the present-day climate (top panel of Figure 10) larger waves are seen off Norway, in the northern North Sea, northwest France, Spain, and the Atlantic coast of Portugal, in contrast to lower waves in the more sheltered southern North Sea and English Channel and at the entrance to the Mediterranean Sea. The future projections of mean SWH (central panel Figure 10) are seen to decrease quite consistently in all four future scenarios, though some increase is projected around the Norwegian coast. The future changes in extreme waves are much more complicated. Overall, larger waves are seen off Norway and the Atlantic coasts of France, Spain, and Portugal. The North Sea displays much more uncertainty between the four futures: here there is no consistent direction of change projected in the future, while the exposed Atlantic-facing coast has a more consistent view of the future with all scenarios projecting increased extreme SWH. This includes the English Channel, which, although it can be considered a semienclosed sea, is exposed to the west to Atlantic storms. These change signals should be contextualized, by considering the shading in Figures 8 and 9. In some locations, for example, the Atlantic coast of the Iberian Peninsula, the end-century changes are larger than the midcentury but in many other locations the midcentury changes are larger. This is probably due to the large interannual to decadal variability in the wave conditions (Wolf et al., 2015).

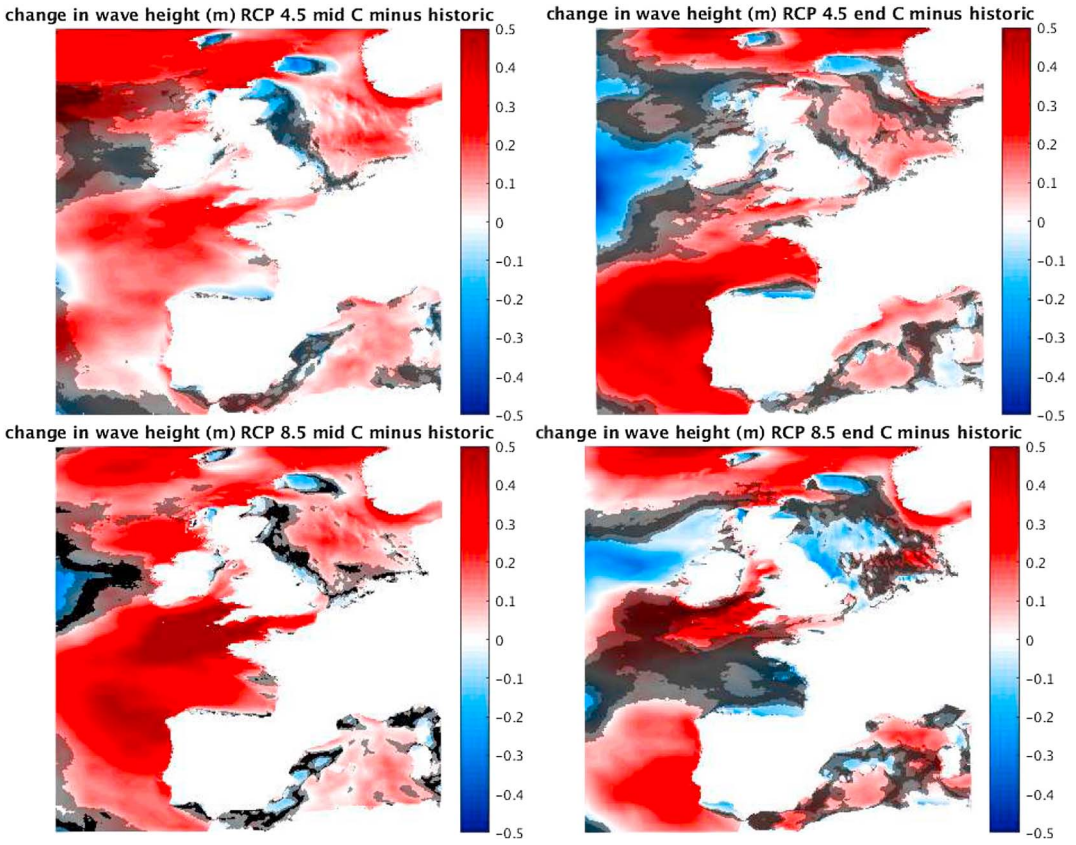

Figure 9. Projected changes in future AnnMax SWH (m). Areas masked in black have a confidence below 50% and those masked in gray a confidence below 75%. (top row) RCP4.5.(bottom) RCP8.5. (left) Middle century. (right) End century. RCP = Representative Concentration Pathway.

Figure 11 shows the same format for the U.K. coast and Figure 12 for the coast of Ireland. Along the U.K. coast, there is a projected decrease in the mean SWH for the majority of the projections. This decrease is largest in the North Sea. Similar to continental Europe (Figure 10), the extreme (AnnMax) wave heights are seen to be much more variable between projections. However, some consistent features emerge. Again, there is a marked contrast between wave heights on the exposed Atlantic coasts and the more sheltered North Sea and Irish Sea. The Atlantic-facing coasts, for example, Cornwall, experience increased extreme SWH in all futures. Increases in wave height are seen in the exposed southwest (English Channel) and northwest approaches (Western Isles of Scotland), whereas more sheltered areas show mixed results, with largest discrepancies between RCPs and time horizons for the east coast of England and Scotland and the Irish Sea. There is no consistent direction of change along the North Sea coast, with RCP4.5 and RCP8.5 forecasting alternately increases/decreases at the same point. When this degree of intermodel variability is observed, any changes may not be statistically significant.

Finally, for the Irish coast (Figure 12), a decrease in mean SWH is seen, of the order of 10% in places. There is little difference around the coast, and the futures show a consistent direction of change. The extreme wave heights follow the same pattern as seen in Figures 10 and 11, with increased spatial variability in future and a complex direction of change. Increases in extreme wave height are seen almost everywhere, except on the east coast of Ireland, facing the Irish Sea, which is sheltered, with fetch-limited growth for westerly winds, like the east coast of the United Kingdom. There is no consistent pattern for whether midcentury or end century produces larger changes and whether RCP8.5 (with larger emissions and larger warming) gives larger changes in wave height, although the midcentury changes, for both RCPs, have a larger increase in mean annual wave height than the end century, for the Atlantic-facing coasts. These results may be compared to Gallagher et al. (2016) which projects a decrease in mean SWH all around Ireland for all seasons. They observe the largest reduction in SWH during the summer months (15% reduction) compared with a decrease of 10% during the winter. However, Gallagher et al. (2016) do not address future changes in high-end waves.

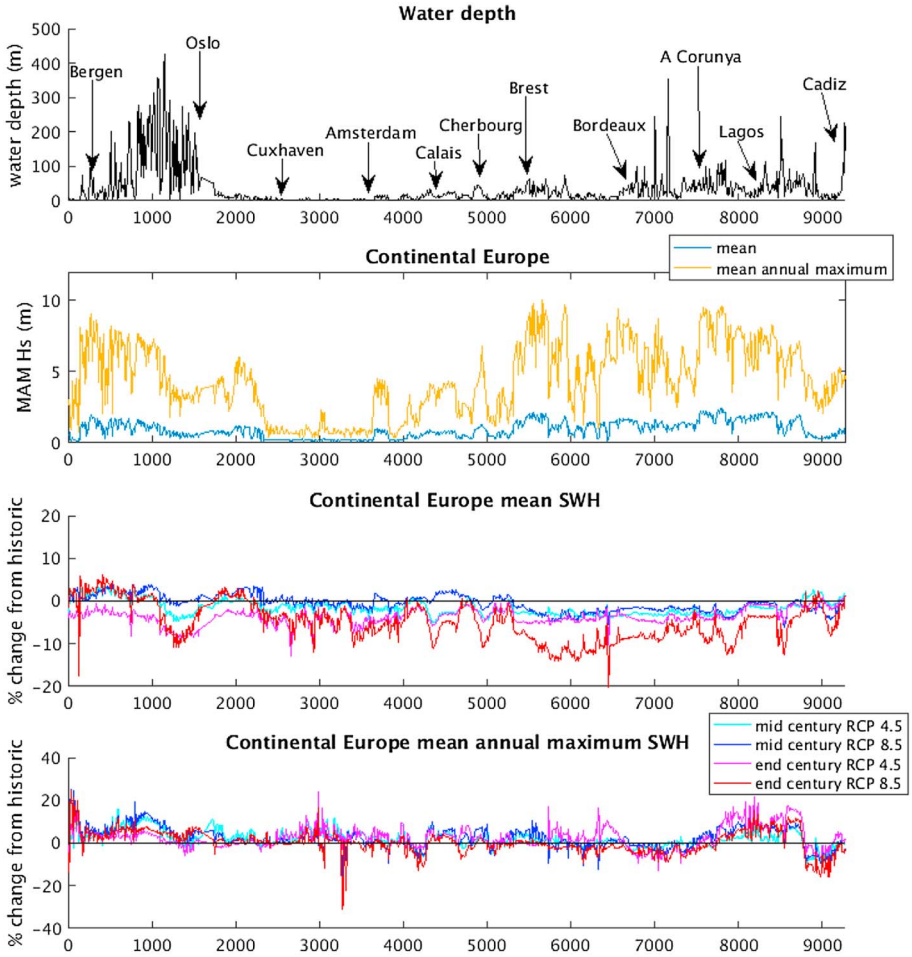

Figure 10. Coastal wave conditions along the continental coast of Europe from Norway to Gibraltar, starting in the NW and moving clockwise, for present-day (1970–1999) and future projections. The first panel shows the modeled water depth, and second panel shows the Mean and AnnMax SWH from the historic run. The third panel shows percentage change in mean wave height and the fourth panel the percentage change in mean annual maximum wave height for midcentury (2030–2059) and end century (2070–2099) for RCP4.5 and RCP8.5. SWH = significant wave height; RCP = Representative Concentration Pathway.

To summarize, a decrease in mean SWH is seen across most coastal areas. These changes are of the order 10%, and there is a largely coherent signal in all future projections (middle/end century and RCP4.5 and 8.5). Future changes in AnnMax SWH are less consistent in direction and coherent between futures. However, there is closer agreement in a prediction of larger extreme waves on Atlantic-facing coasts. The differences between future projections are large in some sea areas, especially those with more moderate wave heights such as the east coast of the United Kingdom, which may be caused by different patterns of wind directions and the changing frequency of westerly winds, possibly leading to more common bimodal sea states. These coastal changes must also be contextualized with the statistical confidence maps (shown by shading in Figures 8 and 9). These show that we have clearer signals of change by the end century (particularly for the mean SWH). The confidence in projected changes in AnnMax is lower, and this is brought out by differences in the possible future conditions, even the trend of future change.

7. Changes in Extreme Waves

The conclusion of sections 5 and 6 is that the mean wave height is predicted to decrease in the future, while the behavior of extreme waves is more complex and seen to increase in places. While in most places the mean SWH decreases with a robust, statistically significant trend, the extreme SWH increases at some sites and decreases in others. If this is the case, the shape of the PDF may be changing, that is, the central estimate can remain the same while the PDF widens and the tail lengthens. When high wave conditions are discussed,

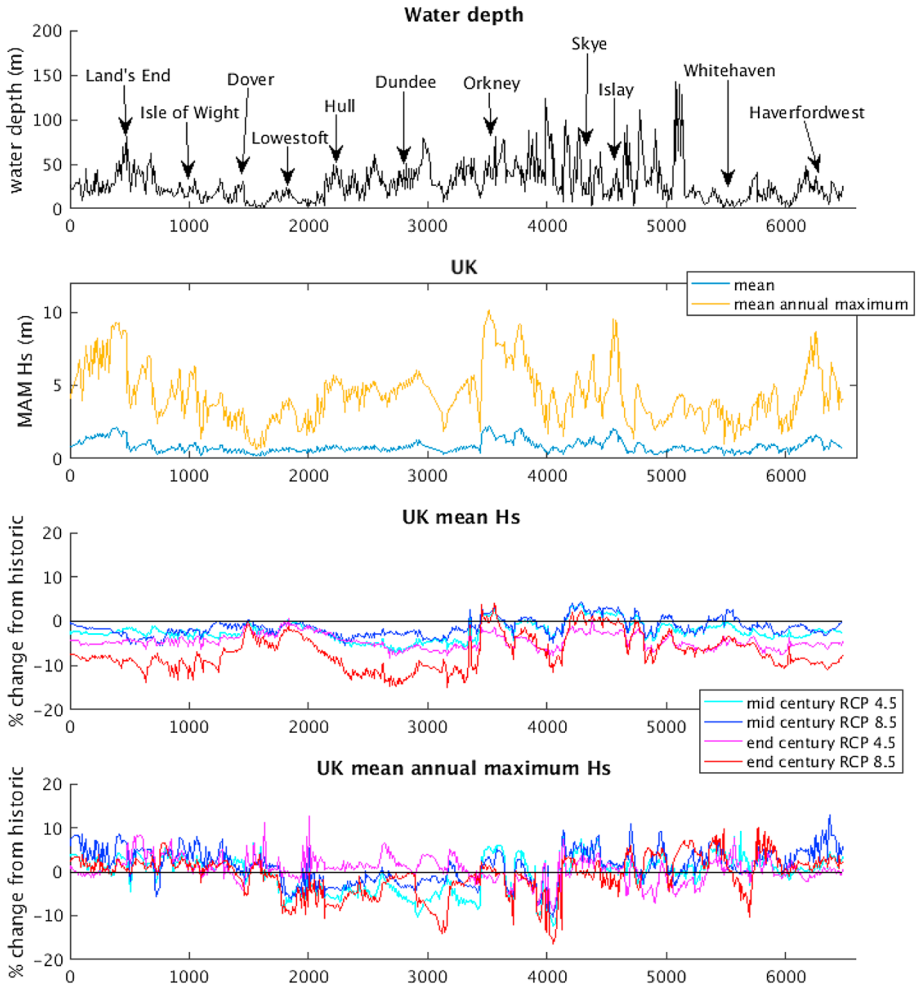

Figure 11. Coastal wave conditions around mainland Great Britain, starting in the Bristol Channel and moving clockwise, for present-day (1970–1999) and future projections. The first panel shows the modeled water depth, and the second panel shows the AnnMax SWH from the historic run. The third panel shows percentage change in mean wave height and the fourth panel the percentage change in mean annual maximum wave height for midcentury (2030–2059) and end century (2070–2099) for RCP4.5 and RCP8.5. SWH = significant wave height; RCP = Representative Concentration Pathway.

different measures of *extreme* waves can be used. Upper percentiles are often referred to as the maximum seasonal or annual wave height. Looking at the historic period, the spatial pattern of the annual maximum and 90th/95th/99th percentile is very similar (not shown). It is only when we examine higher percentiles (e.g., 99.9th) that a different spatial pattern emerges. This result is much more patchy and similar to the annual maximum. We conclude from this that the 90th/95th percentiles are a useful synoptic picture of extreme waves, while the annual maximum and 99.9th percentile better represents a composite picture of individual storm events. Aarnes et al. (2017) also assess different behaviors in the annual maximum and higher percentiles, also seeing more uncertainty and a spatially patchier more variable in the maximum than the 90th percentile. When we compare future changes in extremes with these different measures in our study, we see larger areas of stronger positive change when looking at higher percentiles. The very largest values (maximum, 99.9th percentile) of SWH are seen to increase more than the 95th/99th percentiles. The areas where a positive change is seen (i.e., an increase in high waves rather than a decrease) are also larger when considering the very highest SWH.

To examine this behavior in more detail, the full PDF (computed using hourly data over 30 years) of SWH is extracted at a few selected sites, then normalized. The historical PDF is plotted, together with the two future end-century distributions, on a semilogarithmic scale. By using a logarithmic scale for the PDF, we can focus on the tail which contains infrequent, high SWH events. Figure 13 shows the normalized PDFs for six sites

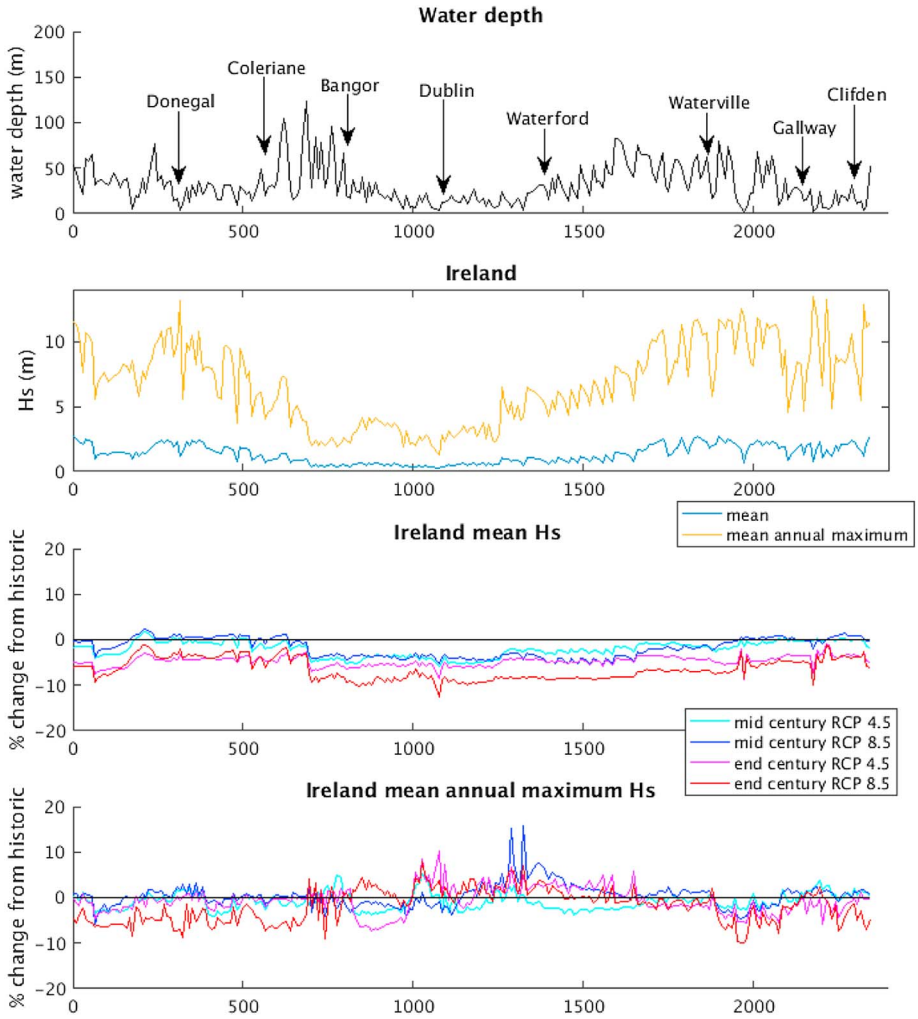

Figure 12. Coastal wave conditions around mainland Ireland, starting in the NW and moving clockwise, for present-day (1970–1999) and future projections. The first panel shows the modeled water depth, and the second panel shows the Mean and AnnMax SWH from the historic run. The third panel shows percentage change in mean wave height and the fourth panel the percentage change in mean annual maximum wave height for midcentury (2030–2059) and end century (2070–2099) for RCP4.5 and RCP8.5. SWH = significant wave height; RCP = Representative Concentration Pathway.

which cover a range of water depths and exposures, with their mean values overlaid as vertical lines. Where the tails of RCP4.5 and RCP8.5 simulations extend beyond the extent of the historical distribution on the *x* axis, larger wave events are seen in future. Where the future curves show a higher (lower) PDF value, these events are more (less) frequent in the RCP simulations compared with the baseline. At the Liverpool site, there is little difference between the simulations and no clear change in the future climate distribution. At the Poole Harbour buoy the value of the largest SWH remains unchanged, while the probability of the large events is seen to increase in both future simulations. In South Knock the RCP4.5 future shows a similar distribution to the historic; however, the RCP8.5 simulation has a decrease in extreme SWH. At the Moray Firth site, there is some suggestion of an increase in large SWH in the RCP4.5 simulation but a reduction observed in the RCP8.5 results. At the Belmullet and west of Hebrides sites there is an increased frequency of large SWH events observed in both future scenarios. The mean SWH (vertical lines in Figure 13) is hardly seen to change at all at these sites, while the extreme waves diverge strongly from the historic conditions in the future.

The tails of the PDF can be examined by looking at the largest SWH of the distributions in more detail. Two populations of SWH can be compared by plotting the historic against the future in a percentile plot (Coles et al., 2001). By plotting the top 99th percentile of the whole population, we can examine the differences between two populations. If the values collapse onto a straight 1:1 line, this suggests that the two sets of sample data

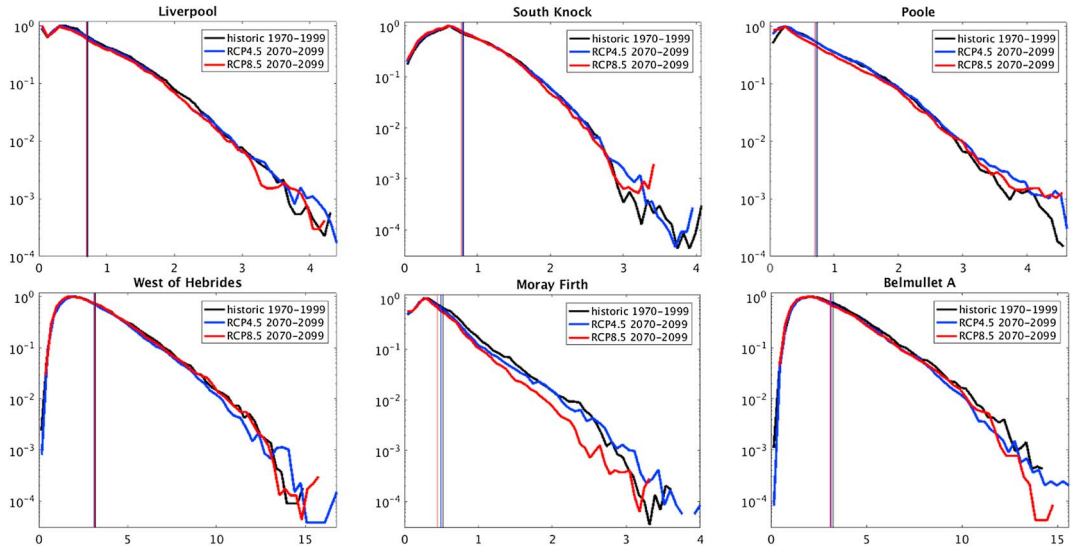

Figure 13. Normalized histograms of significant wave height from six sites. Comparing historical climatology (black) with RCP4.5 (blue) and RCP8.5 (red) end-century futures (*y* axis). The mean of each distribution is plotted as a vertical line, results from the regional model. RCP = Representative Concentration Pathway.

have the same distribution. However, where the fit diverges, the distributions differ in the future compared to the historical waves. This technique is now applied to the 30-year data sets from the historic modeled waves and two future scenarios. In Figure 14 the historic 30-year period is compared with the middle (2030–2059) and end century 30 years (2070–2099) for both RCP4.5 and RCP8.5 scenarios. The 99th percentile is calculated from the hourly SWH for each year then these three values are plotted in Figure 14. By examining the tails of the distribution in this way, we can examine how the most extreme wave conditions may change in the future. From Figure 13 we can see that an increase in the 99th percentile SWH is projected to rise in most future projections at K7, Hebrides, and station 8993 (all to the north of the domain), also at stations 733 and 7336 to the west of Iberia. These increases in extremes are consistent with the AnnMax maps (Figure 9). A decrease in the 99th percentile SWH is projected in the North Sea (sites 8705, South Knock, and Moray Firth) and also to the west of Ireland (K4 and K2); again, these changes are consistent with Figure 9. This visualization yields the same conclusion as considering the full PDF but shows more clearly the absolute changes in future extreme SWH.

To examine changes in very high-end waves, generalized extreme value (GEV) methods can also be used. The *r-largest* approach (Guedes-Soares & Scotto, 2004; Weissman, 1978) is used here to select the largest unique events per year. These events must be separated in time in order that the same storm is not double counted. A range of separation times were tested: from 6 hr and up to 5 days. The confidence of the fit improved on extending the separation to 24 hr. Making the separation time any longer than this did not improve the confidence, while tending to artificially reduce the projected extremes (because it does not consider enough unique events). After choosing the separation time of 24 hr between events, selecting the number of independent large events (*r*) per year is critical. If *r* is too large, bias can occur; if it is too small, the variance and thus uncertainty in the fit can be high. After experimenting with a range of values for *r* (1, 3, 5, 10, 20, 30), 10 events per year were found to be the optimum number. Therefore, as we are considering the wave conditions over a 30-year period, 300 unique values are used per GEV fit. The fit is generated using MATLAB inbuilt software which applies the approach of Embrechts et al. (2013) and Kotz and Nadarajah (2000). Having chosen an appropriate event separation and value of *r*, this method can also be used to extract a return level associated with a particular time period (i.e., the largest expected SWH during a 100-year period). The application of extreme value methods such as this uses a statistical fit to extrapolate outside the length of the available data set. Figure 15 shows the return periods calculated using this method at six buoy sites, color coded by time period as in Figures 10–12. Return levels of SWH are shown for the historic baseline climate and four futures (RCP4.5 middle and end centuries and RCP8.5 middle and end centuries). The GEV curves in Figure 15 show the central estimate of predicted future extreme waves up to the 1 in 100-year event. The GEV fits have associated confidence intervals, which increase in future, indicating more uncertainty in the fit at larger SWH

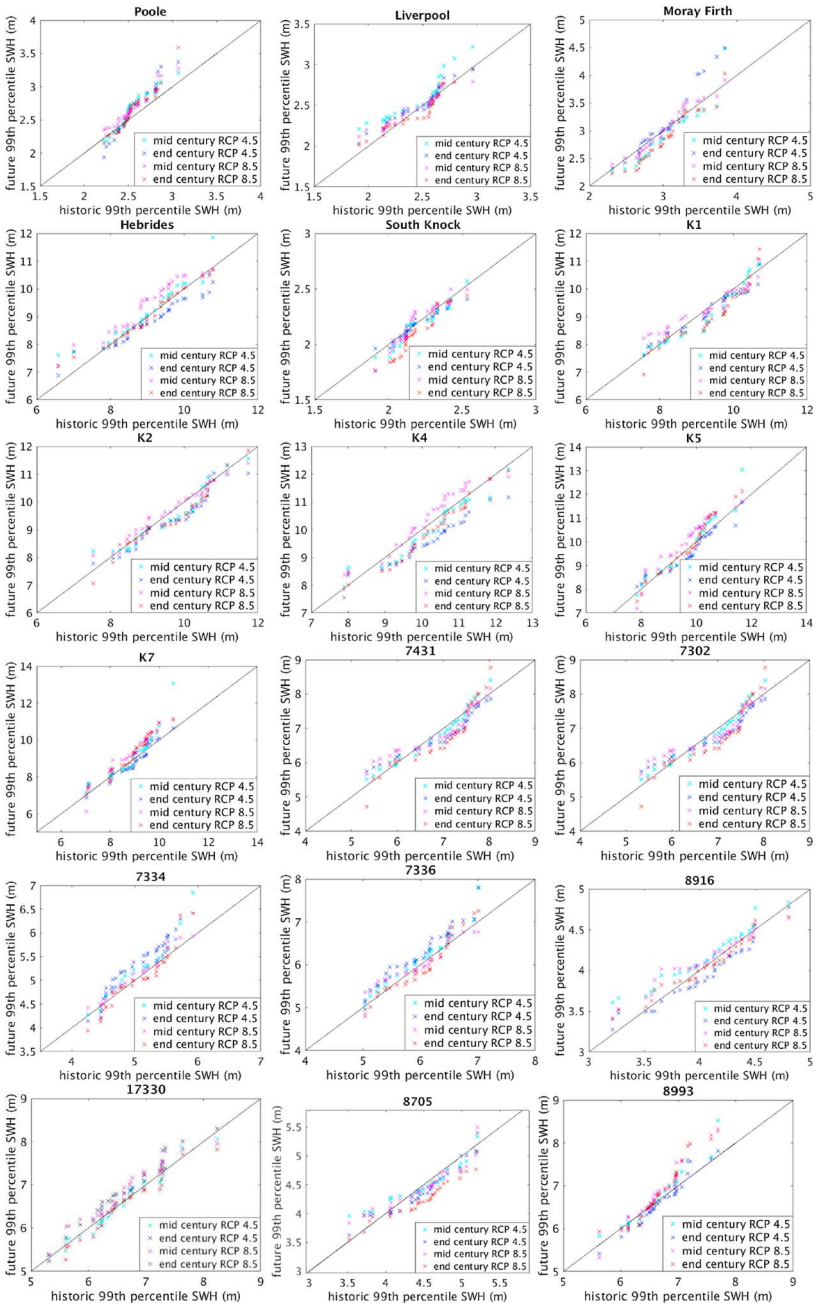

Figure 14. Plots of full 99th percentile of SWH comparing historical climatology (*x* axis) with four future projections (*y* axis), results from the regional model and color coded as for Figures 10–12. SWH = significant wave height; RCP = Representative Concentration Pathway.

return levels. Figure 16 shows the full range of projected extreme SWH for two buoy sites, with the confidence intervals indicated by shading. This shows the difficulty of distinguishing between likely future wave height return levels. The confidence in these projections is low; a similar result is seen at the other sites but not shown further here. The future changes in GEV fit fall within the confidence interval of each future projection, meaning we are unable to draw strong conclusions about future changes in extreme wave conditions. There is an indication, however, that the range of extremes will change in the future. The GEV fit is made up of a location, shape, and scale parameter. The scale parameter (σ) is a measure of the spread, or variability, of the fitted distribution. Table 7 contains the fitted sigma to a subset of six buoys. Poole Harbour, Moray Firth, Belmullet A, and west of Hebrides have a larger spread in the future projections compared to historic conditions. At Liver-

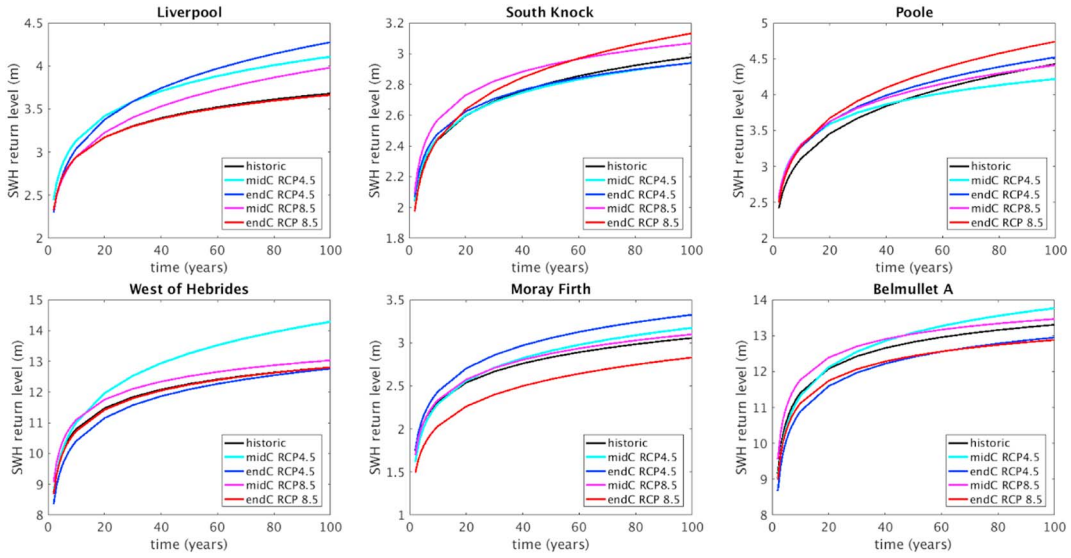

Figure 15. Return value plots of extreme SWH for six sites. Historic results (black), RCP4.5 middle century (cyan), and end century (blue). RCP8.5 middle century (magenta) and end century (red). SWH = significant wave height; RCP = Representative Concentration Pathway.

pool and South Knock there is no consistent change between the four future projections. At the buoys with increased σ values, we conclude that there will be a large range of extreme wave heights in the future.

8. Discussion

To revisit the aims of this work, we first sought to examine where dynamical downscaling may add value to wave projections. The downscaling of the wave model has two parts: (i) a high-resolution wave model, driven by (ii) high-resolution wind forcing. The higher-resolution wave model adds value by better resolving the coastal geometry and water depth. The improved atmospheric resolution may provide a better representation of passing storms and high winds. As well as an improved resolution of available outputs, the dynamical downscaling has been shown to improve wave direction across all observed sites. While downscaling has been clearly shown to improve wave direction and period, there is no clear improvement of the model's representation of SWH during the ERA-Interim run. In fact in some sites the bias between model and observations worsens in the high-resolution model. Returning to the forcing data, this behavior can be directly linked to the wind speeds. Comparing the performance of the modeled winds at the offshore K-buoys, we find that the regional model is more poorly correlated with the observed wind speed (not shown). The global wave model is forced by ERA-Interim (Dee et al., 2011) which is a global atmospheric reanalysis including a four-dimensional variational data assimilation scheme (4D-Var). The regional wave model, however, is forced by ERA-Interim

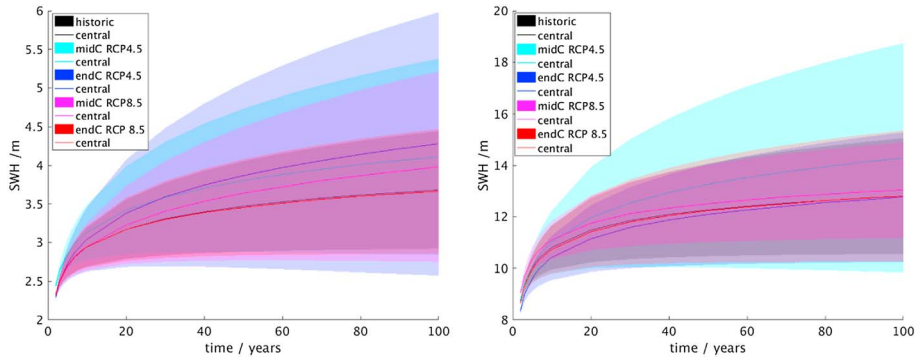

Figure 16. Return value plots of extreme SWH for Liverpool Bay (left) and west of Hebrides (right). The shading denotes the extent of confidence intervals for each extreme value fit. SWH = significant wave height; RCP = Representative Concentration Pathway.

Table 7
Sigma (Spread) Fitted to the 300 r Largest Events

Buoy	Hist	4.5 middle	4.5 end	8.5 middle	8.5 end
Liverpool	0.346	0.338	0.329	0.269	0.343
South Knock	0.199	0.215	0.230	0.278	0.222
Poole	0.287	0.402	0.347	0.351	0.334
W Hebrides	1.287	1.093	1.153	1.275	1.246
Moray	0.295	0.349	0.349	0.349	0.259
Belmullet	1.515	1.333	1.408	1.584	1.451

winds downscaled through a free-running regional EC-Earth climate model. This suggests trade-off between the benefits of higher spatial resolution versus data assimilation. Is it better to have the coarser-resolution winds with better correlations due to the assimilation of observations or better resolved spatial detail, with the atmospheric forcing missing some events? When it comes to future climate runs, this question becomes obsolete, as there is no possibility of data assimilation. We are also interested in the changing wave conditions in a more average, climatological sense rather than representing specific events. The underprediction of the winds for coarse-resolution models is a well-recognized problem, with various bias corrections being suggested (e.g., Brown et al., 2014). Brown et al. (2012) made a comparison of the percentile values, for wind observations at the mouth of the Dee estuary, with the modeled winds at the WaveNet location, for the period 2006–2009, and suggested that the climate model wind distribution is linearly related to observed winds but with increasing underprediction for each percentile. In this study we also see a slight underprediction in the largest modeled SWH (see Figure 3), but the representation of 99th percentile waves is acceptable. As we are interested in relative changes between the historic and future waves forced by the same model, this underprediction is assumed to be present in and consistent across all simulations.

The second aim was to investigate projected future changes in wave conditions. The position and intensity of midlatitude storms drive the wave conditions around NW Europe. Climate models have known biases, particularly in their representation of storm tracks in the North Atlantic. So the question is whether we can distinguish statistically between projections of future wave conditions, with these known uncertainties. We can decompose the total system uncertainty into three parts: natural variability, climate uncertainty, and model uncertainty. To minimize climate model uncertainty, we chose to use the EC-Earth model, which is one of the best performing climate models in terms of representing present-day winter time storm position and median latitude of cyclones. By using a dynamical downscaling approach (see, e.g., Figure 7), we can look at changes in SWH close to the coast, and in semienclosed seas, which are not well represented in global model configurations. This adds value to the projections as the 9-km resolution model is able to better capture the coastline geometry and bathymetry. Value is also added through the use of downscaled atmospheric forcing, which are better able to capture strong wind and low pressures associated with midlatitude cyclones (Mass et al., 2002). To reduce uncertainty in the dynamical wave model, the WW3 configuration has been validated against observations when forced with the best available (ERA-Interim) historic winds. It is important to note that we are only using a single model in this study, and in future these projections must be considered as part of a multimodel ensemble, to properly explore model uncertainty.

To properly address natural variability, very long (multidecadal) observation time series would be required. However, in this work we examine 30-year model time slices, to best eliminate low-frequency variability as was discussed in Wolf et al. (2015). Finally, we turn to the dynamic question of this study, the climate uncertainty, to address the question of whether European wave conditions are changing as a result of global warming. An updated review of the changing climate of the United Kingdom is being prepared (U.K. Climate Predictions 2018; Palmer et al., 2018). This reviews the performance of CMIP5 models for the North Atlantic. Palmer et al. (2018) present an analysis of changing storm track position and storm strength, comparing CMIP3 and CMIP5 models, based on that presented by Wade et al. (2015). There is no clear consensus in the direction of movement in the storm track, or change in strength, but the CMIP5 models cluster more toward a weakening and southward shift, while the older CMIP3 models were clustered around no change (Wade et al., 2015). The North Atlantic storm track is projected to move south and also decrease in strength in the EC-Earth model (Wade et al., 2015). EC-Earth is one of the models which shows this direction of change in storminess most strongly. As the overall decrease in mean SWH projected for the end of the century will be closely linked with

projected changes in North Atlantic storms, therefore, the wave community should closely follow the progress of projects such as CMIP and UKCP providing such assessments.

Though there may still be a degree of uncertainty around the changing wind climate of the north Atlantic, assessing future wave conditions may give some insights to the changing state of the climate. Waves have an integrative effect, which may amplify changes in atmospheric forcing where there is no clear change in wind speed. This is particularly relevant when we come to contrasting the wave conditions at coasts with different exposures. West facing coasts of Europe have a longer fetch and may be dominated by nonlocal swell waves created by storms tracking across the Atlantic. Enclosed areas such as the Irish Sea are fetch limited and dominated by locally generated wind waves. Any changes in future wave conditions at these sites will be driven mainly by the collocated driving winds. When looking for robust signals in the changing wave conditions, we should concentrate on the locations with a longer fetch and examine both wind sea and swell. Bimodal, or mixed, seas have waves generated both locally and nonlocally. This combination of wind sea and swell can be observed on east facing U.K. coastlines, especially the North Sea, depending on wind direction. In the North Sea, westerlies are short fetch but north easterly and south easterly winds can be long fetch. A location with typically multimodal spectra is the Moray Firth. The retreat of sea ice has an impact on the fetch available over which to grow waves. An increased fetch in future projections leads to an increase in both mean and AnnMax sites north of 60°N.

It is important to consider both mean and extreme wave height together, and there are also different measures of extreme waves. While the annual maximum relates directly to events, higher percentiles can give a synoptic view. When we analyze higher and higher percentiles, the number of events included decreases, and thus, the uncertainty increases. A reduction in mean SWH is not incompatible with an increase in extremes, rather, these results suggest that the PDF of wave heights may be widening (leading to longer *tails* in the distributions). Aarnes et al. (2017) also project a decrease in mean SWH of the order of 10% in the Central North Atlantic by the end of the century. They also note that the upper percentiles of future wave height have a higher variance than the mean climate, which is consistent with our findings here. We also find that when looking at future changes in extreme waves, the choice of metric may affect your conclusion. For example, larger areas of strong positive change were identified when using the 99.9th percentile or annual maximum. These changes were not evident when only the 95th or 99th percentile was analyzed.

The uncertainty in future wave projections can be assessed by a statistical analysis. Applying the KW test, we see that the projected reduction in mean wave conditions is more robust than projections of increased extreme waves. Though mean wave height is a useful measure of exposure, extreme wave conditions are of more importance to those working in coastal planning and sea defense. This study has demonstrated a gap in our knowledge: to quantify the long-term natural variability of wave conditions around Europe. However, taking into account the large degree of variability in the wave height around NW Europe, a combination of modeling and statistical analysis helps to reduce the sources of uncertainty and draw some conclusions about how the wave conditions may change in future. We have shown that robust changes emerge in mean and extreme SWH to the north of 60°N, where waves are projected to increase in the north due to reduced sea ice. Mean wave heights are projected to decrease, and extremes increase to the west of Iberia, thought to be caused by a southward shift and weakening of the North Atlantic storm track.

How has this study added to the current state-of-the-art projections? Aarnes et al. (2017) analyzed an ensemble of six CMIP5-forced wave models, finding a consensus in reduction in mean SWH across Northern European seas. They also state that future wave climate is more variable than during the historic period. For UKCP09, Wolf et al. (2015) used the wave model WAM to make projections of future wave height around the U.K. coast. Their results are consistent with a southerly shift in the storm track over the United Kingdom, with increased wave heights observed in the south and reductions to the north of the United Kingdom. Our work shows an overall reduction in the mean wave height but with increased extreme waves on (1) west of Portugal and (2) north of 60°N (related to retreating sea ice). Although only a single model is used in our work, it shows results consistent with the multimodel analysis of other authors (e.g., Aarnes et al., 2017). Gallagher et al. (2016) also projected an overall decrease in annual and seasonal mean SWH around Ireland. Vousdoukas et al. (2017) made wave projections of regional climate change out to 2100, concluding that the variability in wave climate is large, with no clear direction of change. Wolf et al. (2015) also tested where the projections were statistically significant, concluding that changes are robust in the English Channel/southern North Sea, but there is a large degree of uncertainty around projections to the west of Ireland in the North East Atlantic.

We find the projected mean wave height to be more robust than the projected extremes, and there is more certainty of a decreased mean wave height by the end of the century for both RCP future scenarios.

The third aim was to assess how changing wave conditions manifest at the coast. By extracting modeled mean and extreme wave heights in a coastal strip and examining the full PDF of wave heights at selected sites, projected differences in future wave conditions can be examined on a port-by-port basis. This kind of detailed output cannot be produced from a coarse-resolution global model, demonstrating another benefit of the dynamical downscaling. Future change in coastal waves must also be considered together with the maps of model bias and statistical significance. Therefore, strong conclusions about direction of change can only be drawn in areas where a change signal emerges from the large inherent natural variability. A greater understanding of the wave conditions can be gained by examining the full PDF of SWHs, although this has a larger overhead associated with it than considering only the mean or a single percentile. Considering the full PDF and focusing on the upper percentiles, we can make site-specific forecasts of changing extreme wave height, with associated confidence intervals. By understanding the nature of the PDF's changing shape, we can understand the subtleties of a decreasing mean climate in association with increased frequency of extreme events.

9. Conclusion

This study uses a dynamical downscaling approach to make a detailed analysis of historic and future wave conditions around the European Atlantic coast (i.e., ignoring the Mediterranean). Projections of mean and extreme wave conditions have been made out to the year 2100, forced by climate model winds from RCP4.5 and RCP8.5 scenarios. The climate model EC-Earth was selected due to its ability to represent North Atlantic extratropical cyclones with small biases, particularly in winter when the largest waves are generated. The global and regional nested model system has been validated against wave buoy data for a validation period spanning 1979–2015. The validation runs were forced by ERA-Interim reanalysis winds downscaled by the free-running regional model, while the global wave model is forced by the global ERA product, which includes data assimilation. The downscaled run better resolved wave period and direction as well as providing a more spatially detailed result. However, the lack of data assimilation led to some underprediction of SWH in semienclosed seas (where wind waves dominate). The EC-Earth *historic* mean and extreme wave conditions were found to be consistent with the hindcast (ERA-Interim forced) simulations. The seasonal cycle in both mean and extreme SWH is well represented, and there is little difference between the model biases observed in the global and regional wave models. Spatial maps of the model bias show that both models are biased slightly high (of the order 10%), but there is no coherence between the patterns of model bias and projected change.

The CMIP5 model EC-Earth was then used to make projection of future wave conditions, with a focus on western Europe. The changes in mean wave conditions are reasonably homogeneous across the NE Atlantic, with a decrease in mean SWH of the order of 0.2 m (around 5–10%) projected across most of the European coast. An increase in waves to the north of Scotland is also observed, partly caused by a reduction in sea ice due to global warming, leading to increased fetch for northerly winds in Nordic Seas. A southward shift in storm track leads to increased maximum SWH to the west of Portugal and a reduction to the west of Ireland. The future change in extreme waves presented a more complex spatial pattern and higher uncertainty. The projected changes in AnnMax SWH are of the order 10% of the historic conditions: of the order 0.5 m and up to 1.0 m in places; however, there are large areas of uncertainty where future change in extreme waves cannot be separated from the natural variability. This suggests an increased intensity of wave events associated with less frequent but more intense storms in the future.

Next, a local focus was taken, generating a set of high-resolution projections more accessible to coastal planners. Coastal strips show the relative changes in future wave conditions at major cities around the European coast. Here the mean SWH is seen to decrease and the AnnMax SWH to increase on Atlantic-facing coasts where swell waves dominate. There was no clear signal in future change in semienclosed seas, however, where waves are driven by local winds. The 99th percentile analysis gives site-specific information and an absolute measure of projected SWH change. The regional projections show more consistent changes across the 21st Century and RCPs for the more exposed coastline, where remote generation of swell waves dominates SWH. For more sheltered sections of coastline, SWH changes are determined primarily by locally generated waves and therefore local weather *noise* seems to dominate over the climate change signal. We note that projected changes in wave climate are inextricably linked to changes in atmospheric circulation and storminess. Given

the inherent uncertainty in projections of storm track changes and the limited sample size available, the wave projections presented here should be viewed as indicative of the direction of potential future change. However, EC-Earth was found to be the best performing model and representative of future storm track behavior seen in CMIP5 models. The extreme SWH can be examined further by evaluating the full PDF. A widening of the PDF is observed at many locations sites in future. A lengthening tail that represents high SWH suggests more intense storm waves in the future. There are still large uncertainties in the projections of large-return period waves, but the possible range of extreme waves can be bounded, giving a useful picture of future wave conditions around the coast of Europe. Further work is needed to contextualize projections in the long-term natural variability, as well as putting our work into the context of a multimodel ensemble.

Acknowledgments
We acknowledge the World Climate Research Programme's Working Group on Regional Climate and the Working Group on Coupled Modeling, former coordinating body of CORDEX and responsible panel for CMIP5. We also thank Grigory Nikulin of SMHI for making available their model GCM and RCM output. We also acknowledge the Earth System Grid Federation infrastructure, an international effort led by the U.S. Department of Energy's Program for Climate Model Diagnosis and Intercomparison, the European Network for Earth System Modeling and other partners in the Global Organisation for Earth System Science Portals (GO-ESSP). This project has received funding from the European Union's Seventh Programme for Research, Technological Development, and Demonstration under grant agreement FP7-ENV-2013-Two-Stage-603396-RISES-AM-. Authors would also like to thank the reviewers for their time and constructive comments. Model data sets generated from this work can be accessed by contacting the authors directly. In due course, these data will be made available through the Coordinated Ocean Wave Climate Project (COWCLIP) project. For more detail, please see https://www.jcomm.info/cowclip. The work was also supported by NOC's National Capability Programme in ocean modeling.

References

Adaptation Sub-Committee of the Committee on Climate Change (ASC) (2015). Developing H++ climate change scenarios for heat waves, droughts, floods, windstorms and cold snaps. Report produced by the Met Office, University of Reading and CEH for the Adaptation Sub-Committee and to support the second Climate Change Risk Assessment (CCRA). (Tech. rep.): Adaptation Sub-Committee (ASC).

Aarnes, O. J., Reistad, M., Breivik, O., Bitner-Gregersen, E., Eide, L. I., Gramstad, O., et al. (2017). Projected changes in significant wave height towards the end of the 21st century—Northeast Atlantic. *Journal of Geophysical Research: Oceans*, *122*, 3394–3403. https://doi.org/10.1002/2016/JC012521

Barnes, E. A., Slingo, J., & Woollings, T. (2012). A methodology for the comparison of blocking climatologies across indices, models and climate scenarios. *Climatic Dynamics*, *38*, 2467–2481.

Battjes, J. A., & Janssen, J. (1978). Energy loss and set-up due to breaking of random waves. *Coastal Engineering 1978* (pp. 569–587). Hamburg, Germany: American Society of Civil Engineers.

Berens, P. (2009). Circstat: A matlab toolbox for circular statistics. *Journal of Statistical Software*, *31*, 1–21.

Bricheno, L. M., Soret, A., Wolf, J., Jorba, O., & Baldasano, J. M. (2013). Effect of high-resolution meteorological forcing on nearshore wave and current model performance. *Journal of Atmospheric and Oceanic Technology*, *30*(6), 1021–1037.

Brown, S., Murphy, J., Harris, G., & Sexton, D. (2014). Climate projections of future extreme events accounting for modelling uncertainties and historical simulation biases. *Climatic Dynamics*, *43*, 2681–2705.

Brown, J., Souza, A., & Wolf, J. (2010). An 11-year validation of wave-surge modelling in the Irish Sea, using a nested POLCOMS-WAM modelling system. *Ocean modelling*, *33*, 118–128.

Brown, J. M., Wolf, J., & Souza, A. J. (2012). Past to future extreme events in liverpool bay: Model projections from 1960–2100. *Climatic change*, *111*(2), 365–391.

Camus, P., Losada, I., Izaguirre, C., Espejo, A., Menéndez, M., & Pérez, J. (2017). Statistical wave climate projections for coastal impact assessments. *Earth's Future*, *5*(9), 918–933.

Cannaby, H., Palmer, M., Howard, T., Bricheno, L., Calvert, D., Krijnen, J., et al. (2015). Projected sea level rise and changes in extreme storm surge and wave events during the 21st century in the region of Singapore. *Ocean Science*, *12*, 613–632.

Carr, D., Littlefield, R., Nicholson, W., & Littlefield, J. (1987). Scatterplot matrix techniques for large N. *Journal of the American Statistical Association*, *82*(398), 424–436.

Castelle, B., Dodet, G., Masselink, G., & Scott, T. (2018). Increased winter-mean wave height, variability, and periodicity in the Northeast Atlantic over 1949–2017. *Geophysical Research Letters*, *45*, 3586–3596. https://doi.org/10.1002/2017GL076884

Chang, E. K. M., Guo, Y., & Xia, X. (2013). CMIP5 multimodel ensemble projection of storm track change under global warming. *Journal of Geophysical Research: Atmospheres*, *117*, 23118. https://doi.org/10.1029/2012JD018578

Coles, S., Bawa, J., Trenner, L., & Dorazio, P. (2001). *An introduction to statistical modeling of extreme values* (Vol. 208). London: Springer.

Conte, D., & Lionello, P. (2013). Characteristics of large positive and negative surges in the Mediterranean Sea and their attenuation in future climate scenarios. *Global and Planetary Change*, *111*, 159–173.

de Vries, H., Woollings, T., Anstey, J., Haarsma, R. J., & Hazeleger, W. (2013). Atmospheric blocking and its relation to jet changes in a future climate. *Climatic Dynamics*, *41*, 2643.

de Winter, R., Sterl, A., & Ruessink, B. (2013). Wind extremes in the North Sea Basin under climate change: An ensemble study of 12 CMIP5 GCMs. *Journal of Geophysical Research: Atmospheres*, *118*, 1601–1612. https://doi.org/10.1002/jgrd.50147

Dee, D., Uppala, S., Simmons, A., Berrisford, P., Poli, P., Kobayashi, S., et al. (2011). The ERA-Interim reanalysis: Configuration and performance of the data assimilation system. *Quarterly Journal of the Royal Meteorological Society*, *137*, 553–597.

Donat, G. C., Leckebusch, M. G., Pinto, J. G., & Ulbrich, U. (2010). European storminess and associated circulation weather types: Future changes deduced from a multi-model ensemble of GCM simulations. *Climate Research*, *42*(1), 27–43.

Embrechts, P., Klüppelberg, C., & Mikosch, T. (2013). *Modelling extremal events: For insurance and finance* (Vol. 33). Berlin: Springer Science& Business Media.

Flato, G., Marotzke, J., Abiodun, B., Braconnot, P., Chou, S. C., Collins, W. J., et al. (2013). Evaluation of climate models. Climate change 2013: The physical science basis. contribution of working group I to the fifth assessment report of the intergovernmental panel on climate change. *Climate Change*, *2013*(5), 741–866.

Gallagher, S., Gleeson, R., Tiron, E. N. D., McGrath, R., & Dias, F. (2016). Twenty-first century wave climate projections for Ireland and surface winds in the North Atlantic Ocean. *Advances in Science and Research*, *13*, 75–80.

Giorgi, F., & Gutowski, W. J. (2015). Regional dynamical downscaling and the CORDEX initiative. *Annual Review of Environment and Resources*, *40*.

Giorgi, F., Jones, C., & Asrar, G. R. (2009). Addressing climate information needs at the regional level: The CORDEX framework. *World Meteorological Organization (WMO) Bulletin*, *58*(3), 175.

Guedes-Soares, C., & Scotto, M. . (2004). Application of the r largest-order statistics for long-term, predictions of significant wave height. *Coastal Engineering*, *51*, 387–394.

Haarsma, R. J., Hazeleger, W., Severijns, C., de Vries, H., Sterl, A., Bintanja, R., et al. (2013). More hurricanes to hit western Europe due to global warming. *Geophysical Research Letters*, *40*, 1783–1788. https://doi.org/10.1002/grl.50360

Harvey, B. J., Shaffrey, L. C., Woollings, T. J., Zappa, G., & Hodges, K. I. (2012). How large are projected 21st century storm track changes? *Geophysical Research Letters*, *39*, L18707. https://doi.org/10.1029/2012GL052873

Hazeleger, W., Wang, X., Severijns, C., Ștefănescu, S., Bintanja, R., Sterl, A., et al. (2012). EC-Earth v2. 2: Description and validation of a new seamless Earth system prediction model. *Climate dynamics*, *39*(11), 2611–2629.
Hemer, M. A., Fan, Y., Mori, N., Semedo, A., & Wang, X. L. (2013). Projected changes in wave climate from a multi-model ensemble. *Nature climate change*, *3*(5), 471–476.
Hemer, M. A., & Trenham, C. E. (2016). Evaluation of a CMIP5 derived dynamical global wind wave climate model ensemble. *Ocean Modelling*, *103*, 190–203.
IPCC, Stocker, T. F., Qin, D., Plattner, G.-K., Alexander, L. V., Allen, S. K., Bindoff, N. L., et al. (2013). Technical Summary, *Climate change 2013: The Physical Science Basis. Contribution of Working Group I to the Fifth Assessment Report of the Intergovernmental Panel on Climate Change* (pp. 33–115). Cambridge: Cambridge University Press.
Jevrejeva, S., Matthews, A., & Slangen, A. (2017). The twentieth-century sea level budget: Recent progress and challenges. *Surveys in Geophysics*, *38*(1), 295–307.
Kjellström, E., Nikulin, G., Strandberg, G., Christensen, O. B., Jacob, D., Keuler, K., et al. (2018). European climate change at global mean temperature increases of 1.5 and 2 °C above pre-industrial conditions as simulated by the EURO-CORDEX regional climate models. *Earth System Dynamics*, *9*(2), 459–478.
Kotlarski, S., Keuler, K., Christensen, O. B., Colette, A., Déqué, M., Gobiet, A., et al. (2014). Regional climate modeling on european scales: A joint standard evaluation of the euro-cordex rcm ensemble. *Geoscientific Model Development*, *7*(4), 1297–1333.
Kotz, S., & Nadarajah, S. (2000). Extreme value distributions: Theory and applications. World Scientific.
Kruskal, W., & Wallis, W. (1952). Use of ranks in one-criterion variance analysis. *Journal of Applied Mathematics and Mechanics*, *47*, 583–621.
Kunz, M., Mohr, S., Rauthe, M., Lux, R., & Kottmeier, C. (2010). Assessment of extreme wind speeds from regional climate models-part 1: Estimation of return values and their evaluation. *Natural Hazards and Earth System Sciences*, *10*(4), 907.
Lionello, P., Conte, D., Marzo, L., & Scarascia, L. (2017). The contrasting effect of increasing mean sea level and decreasing storminess along the coast of the Mediterranean Sea in the mid 21st century. *Global and Planetary Change*, *151*, 80–91.
Lionello, P., & Giorgi, F. (2007). Winter precipitation and cyclones in the Mediterranean Region: Future climate scenarios in a regional simulation. *Advances in Geosciences*, *12*, 153–158.
Lionello, P., & Sanna, A. (2005). Mediterranean wave climate variability and its links with NAO and Indian monsoon. *Climate Dynamics*, *26*, 611–623.
Madec, G. (2008). *NEMO reference manual, ocean dynamic component: NEMO-OPA*. Institut Pierre Simon Laplace: Note du Pole de modélisation.
Mardia, K. V., & Jupp, P. E. (2009). *Directional statistics* (Vol. 494). Chichester, UK: John Wiley.
Marechal, D. (2004). Soil-based approach to rainfall-runoff modelling in un-gauged catchments for England and Wales (Ph.D. thesis), Cranfield University.
Masato, G., Hoskins, B. J., & Woollings, T. (2013). Winter and summer Northern Hemisphere blocking in CMIP5 models. *Journal of Climate*, *26*, 7044–7059.
Mass, C., Owens, D., Westrick, K., & Colle, B. (2002). Does increasing horizontal resolution produce more skillful forecasts? *Bulletin of the American Meteorological Society*, *83*, 407–430.
McGranahan, G., Balk, D., & Anderson, B. (2007). The rising tide: Assessing the risks of climate change and human settlements in low elevation coastal zones. *Environment and urbanization*, *19*(1), 17–37.
Melet, A., Meyssignac, B., Almar, R., & Le Cozannet, G. (2018). Under-estimated wave contribution to coastal sea-level rise. *Nature Climate Change*, *8*(3), 234.
Menendez, M., García-Díez, M., Fita, L., Fernández, J., Méndez, F., & Gutiérrez, J. (2014). High-resolution sea wind hindcasts over the Mediterranean area. *Climate dynamics*, *42*(7-8), 1857–1872.
Mentaschi, L., Vousdoukas, M. I., Voukouvalas, E., Dosio, A., & Feyen, L. (2017). Global changes of extreme coastal wave energy fluxes triggered by intensified teleconnection patterns. *Geophysical Research Letters*, *44*, 2416–2426. https://doi.org/10.1002/2016GL072488
Mizuta, R. (2012). Intensification of extratropical cyclones associated with the polar jet change in the CMIP5 global warming projections. *Geophysical Research Letters*, *39*, L19707. https://doi.org/10.1029/2012GL053032
Moss, R. H., Edmonds, J. A., Hibbard, K. A., Manning, M. R., Rose, S. K., Van Vuuren, D. P., et al. (2010). The next generation of scenarios for climate change research and assessment. *Nature*, *463*(7282), 747–756.
Noye, B. J., Matthews, K., & Grzechnik, M. P. (1999). A three-dimensional model of tides and surges in the Great Australian Bight. In *Modelling Coastal Sea Processes* (Vol. 107–134).
Palmer, T., & Hagedorn, R. (2006). *Predictability of weather and climate*. Cambridge: Cambridge University Press.
Palmer, M., Howard, T., Tinker, J., Lowe, J., Bricheno, L., Calvert, D., et al. (2018). UK climate predictions 2018 (UKCP18) marine report: Met Office.
Palmer, T., Nicholls, R., Wells, N., Saulter, A., & Mason, T. (2014). Identification of 'energetic' swell waves in a tidal strait. *Continental Shelf Research*, *88*, 203–215.
Perez, J., Menendez, M., Mendez, F., & Losada, I. (2014). Evaluating the performance of CMIP3 and CMIP5 global climate models over the north-east Atlantic region. *Climate Dynamics*, *43*, 2663–2680.
Rosen, C. (2000). *World Resources 2000-2001: People and ecosystems: The fraying web of life*. Amsterdam: Elsevier.
Sen Gupta, A., Jourdain, N. C., Brown, J. N., & Monselesan, D. (2013). Climate drift in the CMIP5 models. *Journal of Climate*, *26*(21), 8597–8615.
Strandberg, G., Bärring, L., Hansson, U., Jansson, C., Jones, C., Kjellström, E., et al. (2015). CORDEX scenarios for Europe from the Rossby Centre regional climate model RCA4. SMHI.
Taylor, K., Stouffer, R. J., & Meehl, G. A. (2012). An overview of CMIP5 and the experiment design. *Bulletin of the American Meteorological Society*, *93*, 485–498.
Tolman, H. (2003). Treatment of unresolved islands and ice in wind wave models. *Ocean modelling*, *5*, 219–231.
Tolman, H. (2009). User manual and system documentation of WAVEWATCH III-version 3.14 (Tech. rep.): NOAA / NWS / NCEP / MMAB Technical Note-276.
Tolman, H. L., & Chalikov, D. V. (1996). Source terms in a 3rd generation wind-wave model. *Journal of Physical Oceanography*, *26*, 2497–2510.
Tucker, M. J., & Pitt, E. G. (2001). *Waves in ocean engineering* (Vol. 5). Amsterdam; New York: Elsevier.
Vousdoukas, M. I., Mentaschi, L., Voukouvalas, E., Verlaan, M., & Feyen, L. (2017). Extreme sea levels on the rise along Europe's coasts. *Earth's Future*, *5*, 304–323. https://doi.org/10.1002/2016EF000505
Wade, S. D., Rance, J., & Reynard, N. (2013). The UK climate change risk assessment 2012: Assessing the impacts on water resources to inform policy makers. *Water Resources Management*, *27*(4), 1085–1109.

Wade, S., Sanderson, M., Golding, N., Lowe, J., Betts, R., Reynard, N., et al. (2015). Developing H++ climate change scenarios for heat waves, droughts, floods, windstorms and cold snaps. Committee on Climate Change.

Weissman, I. (1978). Estimation of parameters and large quantiles based on the k largest observations. *American Statistical Association*, *73*, 812–815.

Wolf, J. (2009). Coastal flooding: Impacts of coupled wave–surge–tide models. *Natural Hazards*, *49*(2), 241–260.

Wolf, J., Brown, J. M., & Howarth, M. (2011). The wave climate of Liverpool Bay—Observations and modelling. *Ocean Dynamics*, *61*, 639–655.

Wolf, J., Lowe, J., & Howard, T. (2015). *Broad scale coastal simulation: New techniques to understand and manage shorelines in the third millennium*. Dordrecht: Springer.

Wolf, J., & Woolf, D. K. (2006). Waves and climate change in the north-east Atlantic. *Geophysical Research Letters*, *33*, L06604. https://doi.org/10.1029/2005GL025113

Woollings, T. (2010). Dynamical influences on European climate: An uncertain future. *Philosophical Transactions of the Royal Society of London, A*, *368*, 3733–3756.

Woollings, T., & Blackburn, M. (2012). The North Atlantic jet stream under climate change and its relation to the NAO and EA patterns. *Journal of Climate*, *25*, 886–902.

Zacharioudaki, A., Pan, S., Simmonds, D., Magar, V., & Reeve, D. E. (2011). Future wave climate over the west-European shelf seas. *Ocean Dynamics*, *61*(6), 807.

Zappa, G., Hoskins, B., & Shepherd, T. (2015). Improving climate change detection through optimal seasonal averaging: The case of the North Atlantic jet and European precipitation. *Journal of Climate*, *28*, 6381–6397.

Zappa, G., Masato, G., Shaffrey, L., Woollings, T., & Hodges, K. (2014). Linking Northern Hemisphere blocking and storm track biases in the CMIP5 climate models. *Geophysical Research Letters*, *41*, 135–139. https://doi.org/10.1002/2013GL058480

Zappa, G., Shaffrey, L., & Hodges, K. (2013). The ability of CMIP5 models to simulate North Atlantic extratropical cyclones. *Journal of Climate*, *26*, 5379–5396.

Zappa, G., Shaffrey, L. C., Hodges, K. I., Sansom, P. G., & Stephenson, D. (2013). A multimodel assessment of future projections of North Atlantic and European extratropical cyclones in the CMIP5 climate models. *Journal of Climate*, *26*, 5846–5862.